

The Chemistry of Tetrakis(trifluoromethyl)cyclopentadienone

Mark J. Burk,* Joseph C. Calabrese, Fredric Davidson, Richard L. Harlow, and D. Christopher Roe

Contribution No. 5648 from the Central Research & Development Department, E. I. Du Pont de Nemours & Company, Experimental Station, Wilmington, Delaware 19880-0328.

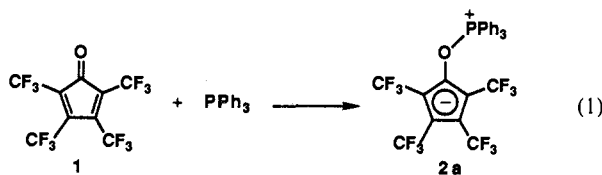
Received September 17, 1990

Abstract: Studies aimed at understanding the reactivity of tetrakis(trifluoromethyl)cyclopentadienone (TTFC, **1**) are reported. Reactions between **1** and phosphines were found to afford the kinetic adducts **3** which arise from regioselective nucleophilic addition of PR_3 to the carbon adjacent to the carbonyl group of TTFC. Thermolysis of solutions containing **3** resulted in facile C to O rearrangement of PR_3 and yielded the thermodynamic ylides **2**. Irradiation of the thermodynamic ylides **2** led to photoreversion back to the kinetic adducts **3**. Mechanistic studies indicate that these rearrangements proceed through a dissociative pathway involving P-C (thermal) or P-O (photochemical) bond heterolysis. Fluoride reacted with TTFC in a similar regioselective fashion to give the adduct **5**. By using magnetization transfer techniques, we have discovered a rare example of what is formally a reversible 1,3-fluorine migration in **5**. Nucleophiles containing protons attached to the heteroatoms (HX) yielded products (**6**) derived from formal addition of HX across one of the C=C double bonds of **1**. One-electron reduction of TTFC provided the stable radical anion salt **12**, while electrochemical studies showed a reversible one-electron reduction wave at $E_{1/2} = +0.37$ V (vs SCE) for **1**. Chemical reduction of TTFC with trialkylsilanes afforded siloxydienes which could be deprotonated to give the corresponding trifluoromethyl-substituted cyclopentadienide salts (**16-18**) in good yields. The possible intervention of a single-electron-transfer mechanism in nucleophilic addition reactions involving **1** is discussed.

Introduction

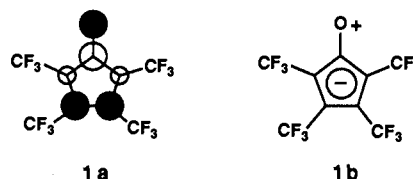
Polyfluorinated molecules often display unique reactivity and solubility properties relative to their nonfluorinated analogues and have been the object of considerable interest for many years.¹ In 1963 Wilkinson and Dickson² reported the discovery of tetrakis(trifluoromethyl)cyclopentadienone (TTFC, **1**), which was prepared by the coupling of hexafluoro-2-butyne and CO in the presence of $[\text{Rh}(\text{CO})_2\text{Cl}]_2$. Given the expected high reactivity of **1**, it is somewhat surprising that relatively few studies involving this compound have been reported. The ability of **1** to form 1:1 charge-transfer complexes with numerous aromatic hydrocarbons was demonstrated by Wilkinson and Dickson,³ while Lemal showed that **1** behaves as a versatile Diels-Alder diene.⁴

Our initial interest in tetrakis(trifluoromethyl)cyclopentadienone (**1**) derived from our desire to synthesize cyclopentadienyl groups bearing multiple trifluoromethyl substituents and to use these as ligands for transition metals; we viewed **1** as a precursor to such ligand systems.⁵ Important in this regard was a report by Wilkinson and Roundhill⁶ describing the isolation of ylide **2a** from the reaction between **1** and PPh_3 (eq 1). The direct formation



of **2a** in this reaction appeared reasonable based on the expected lowering in energy of the cyclopentadienone LUMO **1a** by the trifluoromethyl groups and given the large orbital coefficients on

the carbonyl group.⁴ In more classical terms, an increased contribution of the resonance form **1b** may result from the great anion stabilizing effect of the powerfully electron-withdrawing CF_3 groups. Reverse polarization of the carbonyl group of **1** is thought



to result in nucleophilic attack by PPh_3 at the electrophilic oxygen atom to generate a stable aromatic cyclopentadienide (**2a**), rather than attack in the usual Michael fashion.⁶ Such reactivity indicated that a number of nucleophiles, in addition to phosphines, could be used in a similar manner to provide directly from **1** a series of new tetrakis(trifluoromethyl)cyclopentadienides. Furthermore, we viewed the phosphine oxide moiety of **2a** as a potentially good leaving group in the synthesis of deoxycyclopentadienyl derivatives.

In the course of our studies involving **1**, we have uncovered a wide range of reactivity associated with this molecule. Herein, we wish to report our results which include a reinvestigation of nucleophilic addition to **1**, reaction with proton-containing nucleophiles, cyclopropane formation, one-electron reduction leading to the stable radical anion salt of **1**, and finally chemical reduction with silanes to yield siloxydienes which, upon deprotonation, afford new tetrakis(trifluoromethyl)cyclopentadienyl derivatives.

Results

In accord with the findings of Wilkinson and Dickson,^{2,3} hexafluoro-2-butyne (10 equiv/Rh) and CO (100 atm) reacted in the presence of $[\text{Rh}(\text{CO})_2\text{Cl}]_2$ at 150 °C to afford **1** over 24 h. Sublimation (0.1 Torr, 25 °C) of the obtained brown residue onto a -5 °C cold finger yielded volatile yellow crystals of **1**; thus by using 8 g of $[\text{Rh}(\text{CO})_2\text{Cl}]_2$, 80 g of **1** were obtained. We have observed that **1** is somewhat moisture-sensitive and is best stored below 0 °C under N_2 . Although extremely reactive, **1** is seemingly unaffected by a number of solvents. In addition to acyclic and chlorinated hydrocarbons,³ we have found that Et_2O , CH_3CN , CH_3NO_2 , and glyme are suitable solvents.

The IR spectrum of **1** displayed two intense absorptions at 1755 and 1675 cm^{-1} . The expected isotopic red-shift of 39 cm^{-1} from 1755 to 1716 cm^{-1} was observed for the C=O stretch of ^{13}C -

(1) (a) Chambers, R. D. *Fluorine in Organic Chemistry*; John Wiley and Sons, Inc.: New York, 1973. (b) Banks, R. E. *Fluorocarbons and Their Derivatives*; Oldbourne Book Co. Ltd.: London, England, 1964. (c) Smart, B. E. In *The Chemistry of Functional Groups, Supplement D*; Patai, S., Rappaport, Z., Eds.; John Wiley and Sons, Ltd.: Chichester, 1983; Part 2, Chapter 14, pp 603-655. (d) Riess, J. G.; Le Blanc, M. *Angew. Chem., Int. Ed. Engl.* **1978**, *17*, 621.

(2) Dickson, R. S.; Wilkinson, G. *Chem. Ind.* **1963**, 1432.

(3) Dickson, R. S.; Wilkinson, G. *J. Chem. Soc.* **1964**, 2699.

(4) Szilagy, S.; Ross, J. A.; Lemal, D. M. *J. Am. Chem. Soc.* **1975**, *97*, 5586.

(5) Burk, M. J.; Arduengo, A. J., III; Calabrese, J. C.; Harlow, R. L. *J. Am. Chem. Soc.* **1989**, *111*, 8938.

(6) Roundhill, D. M.; Wilkinson, G. *J. Org. Chem.* **1970**, *35*, 3561.

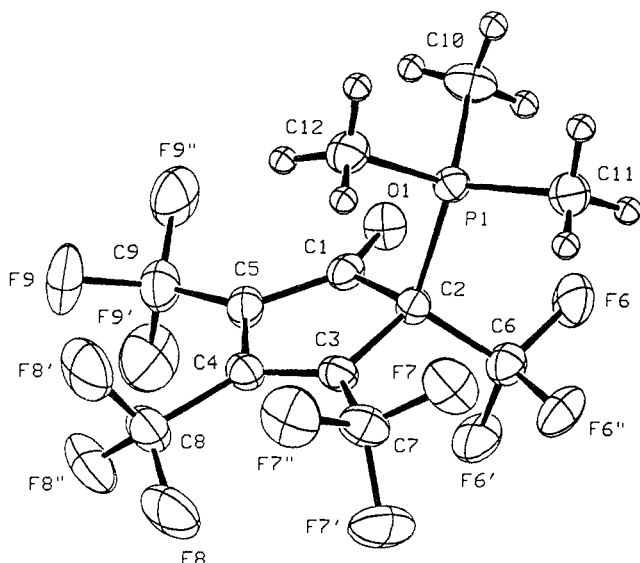
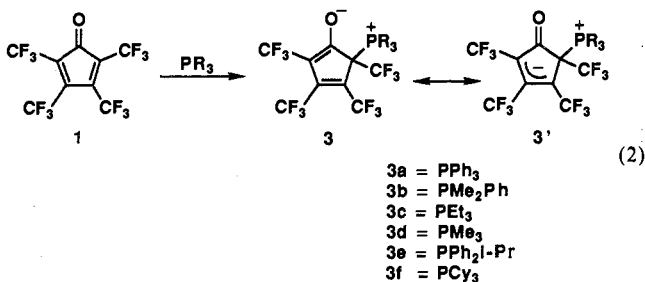


Figure 1. ORTEP plot of PMe_3 adduct **3d** with thermal ellipsoids drawn at the 50% probability level.

labeled **1** (prepared with ^{13}C O), thus allowing definitive assignment of this absorption. Bromination studies previously led Wilkinson and Dickson³ to assign the 1675-cm^{-1} absorption as a $\text{C}=\text{C}$ stretch.

Nucleophilic Addition. (a) **Phosphines.** Reaction between **1** and PMe_2Ph at 25°C in CH_2Cl_2 afforded an adduct identified as the betaine-like zwitterion **3b** (eq 2). Particularly informative



in the characterization of **3b** was the ^{19}F NMR spectrum which displayed four separate signals for the chemically inequivalent CF_3 groups at δ -47.0, -54.9, -58.5, and -59.9 (relative to CFCl_3). Detailed examination of the F-F and P-F coupling patterns suggested the regiochemistry shown for **3b**. The ^{31}P NMR resonance of **3b** at δ 27.6 is characteristic for phosphonium salts derived from PMe_2Ph .⁷ The downfield chemical shift observed in the ^{13}C NMR spectrum for the carbonyl carbon (δ 175.4) of **3b** indicates significant double bond ($\text{C}=\text{O}$) character and suggests that some negative charge lies within the ring containing the electron-withdrawing CF_3 groups (resonance form **3'**). The IR spectrum of **3b** exhibits a $\text{C}=\text{O}$ stretch at 1653 cm^{-1} , while ^{13}C -labeled **3b** shows the corresponding absorption at 1618 cm^{-1} .

In a similar fashion, the phosphine adducts **3c** and **3d** were formed upon reaction between **1** and PEt_3 and PMe_3 , respectively (eq 2). The thermally sensitive analogues **3e** and **3f** were isolated by treating **1** in Et_2O at -30°C with $\text{PPh}_2\text{-}i\text{-Pr}$ and PCy_3 , respectively; the products formed as yellow precipitates which were filtered and stored at -30°C . Consistent with the results of Wilkinson and Roundhill,⁶ no PPh_3 adduct analogous to **3** could be isolated, and only the ylide **2a** was obtained under the conditions described above. By performing the reaction between PPh_3 and **1** at low temperature (-80°C), however, we were able to directly observe by ^{19}F and ^{31}P NMR spectroscopy the initially formed species **3a**. The ^{19}F NMR spectrum of **3a** showed the presence

Table I. Selected Interatomic Distances (\AA) and Intramolecular Angles (deg) for PMe_3 Adduct **3d**

Interatomic Distances (\AA)			
P(1)-C(2)	1.862 (2)	F(9)-C(9)	1.342 (3)
P(1)-C(10)	1.786 (2)	F(9')-C(9)	1.342 (3)
P(1)-C(11)	1.787 (2)	F(9'')-C(9)	1.340 (3)
P(1)-C(12)	1.780 (2)	O(1)-C(1)	1.237 (2)
F(6)-C(6)	1.337 (3)	C(1)-C(2)	1.587 (3)
F(6')-C(6)	1.332 (2)	C(1)-C(5)	1.394 (3)
F(6'')-C(6)	1.333 (2)	C(2)-C(3)	1.519 (3)
F(7)-C(7)	1.343 (3)	C(2)-C(6)	1.525 (3)
F(7')-C(7)	1.348 (3)	C(3)-C(4)	1.355 (3)
F(7'')-C(7)	1.337 (3)	C(3)-C(7)	1.484 (3)
F(8)-C(8)	1.336 (3)	C(4)-C(5)	1.434 (3)
F(8')-C(8)	1.321 (3)	C(4)-C(8)	1.511 (3)
F(8'')-C(8)	1.328 (3)	C(5)-C(9)	1.474 (3)

Intramolecular Angles (deg)			
C(2)-P(1)-C(10)	110.9 (1)	C(1)-C(2)-C(3)	102.6 (2)
C(2)-P(1)-C(11)	113.4 (1)	C(1)-C(2)-C(6)	107.5 (2)
C(2)-P(1)-C(12)	106.8 (1)	C(3)-C(2)-C(6)	113.9 (2)
C(10)-P(1)-C(11)	106.7 (1)	C(2)-C(3)-C(4)	108.1 (2)
C(10)-P(1)-C(12)	108.9 (1)	C(2)-C(3)-C(7)	124.3 (2)
C(11)-P(1)-C(12)	110.2 (1)	C(4)-C(3)-C(7)	127.5 (2)
P(1)-C(2)-C(1)	105.9 (1)	C(3)-C(4)-C(5)	113.1 (2)
P(1)-C(2)-C(3)	113.6 (1)	C(3)-C(4)-C(8)	125.0 (2)
P(1)-C(2)-C(6)	112.2 (1)	C(5)-C(4)-C(8)	121.9 (2)
O(1)-C(1)-C(2)	121.3 (2)	C(1)-C(5)-C(4)	109.1 (2)
O(1)-C(1)-C(5)	132.1 (2)	C(1)-C(5)-C(9)	121.1 (2)
C(2)-C(1)-C(5)	106.6 (2)	C(4)-C(5)-C(9)	129.6 (2)

of four inequivalent CF_3 groups at δ -47.2, -54.6, -55.3, and -60.1, while the ^{31}P resonance appeared at δ 23.1. Products derived from PR_3 attack at the β -carbon were never observed in reactions between **1** and phosphines.

The molecular structure of the PMe_3 adduct **3d** was firmly established by X-ray crystallography, and the ORTEP diagram is shown in Figure 1. Suitable crystals were obtained by slow crystallization from $\text{THF}/\text{Et}_2\text{O}$ at -40°C . The regiochemistry of kinetic phosphine addition to the α -carbon of **1** was confirmed. Selected interatomic bond distances and intramolecular angles are listed in Table I. The five-membered ring of **3d** remains reasonably planar, and C2 deviates by only 0.093 \AA from the plane of the other four carbon atoms. The P1-C2 bond distance (1.86 \AA) is considerably longer than the P-C(methyl) bond lengths (av 1.78 \AA). Steric interactions between PMe_3 and adjacent CF_3 groups apparently result in ground-state weakening of this bond. Such bond weakening in the adducts **3** may be responsible for the observed kinetic lability of these compounds (vide infra). The C-O bond length of **3d** (1.20 \AA) is close to that expected for a carbonyl double bond of this sort⁸ and further indicates that some negative charge may be delocalized within the ring of **3**. The C-C bond distances of the five-membered ring, however, suggest that the dienolate form **3** (rather than **3'**) may best represent the electronic structure of these molecules. The short distances C3-C4 (1.355 \AA) and C1-C5 (1.394 \AA) indicate the presence of C-C multiple bonds which are separated by the relatively longer bond C4-C5 (1.434 \AA). These structural features led us to depict the kinetic adducts **3** in the dienolate form rather than the delocalized form (**3'**) throughout the remainder of the paper. We also have determined the structure of the PMe_2Ph adduct **3b** by X-ray diffraction methods. While the quality of the data was sufficient to allow assignment of molecular structure (**3b** is essentially isostructural with **3d**), disorder in the crystal hampered the refinement which converged at $R = 7.3\%$, $R_w = 5.8\%$, and no topographical features will be reported.

Thermal Rearrangement. Allowing a solution containing the PPh_3 adduct **3a** to warm from -80°C to -30°C led to complete rearrangement to the thermodynamic ylide **2a**, as evidenced by the appearance of a new pair of ^{19}F resonances at δ -49.9 and -50.7, along with a new ^{31}P resonance at δ 68.4. Likewise,

(7) Tebby, J. C. In *Phosphorus-31 NMR Spectroscopy in Stereochemical Analysis*; Verkade, J. G., Quin, L. D., Eds.; VCH Publishers, Inc.: Deerfield Beach, FL, 1987; Chapter 1.

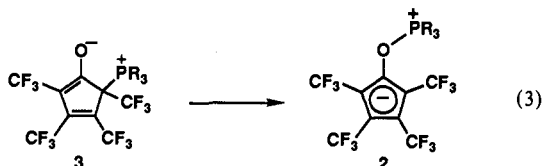
(8) (a) Bailey, N. A.; Mason, R. *Acta Crystallogr.* **1966**, *19*, 652. (b) Gerloch, M.; Mason, R. *Proc. Roy. Soc. A* **1964**, *279*, 170.

Table II. Selected Interatomic Distances (Å) and Intramolecular Angles (deg) for Thermodynamic Ylide **2b** (Extended Isomer, Figure 2A)

Interatomic Distances (Å)			
P(1)–O(1)	1.584 (2)	O(1)–C(1)	1.409 (4)
P(1)–C(10)	1.770 (3)	C(1)–C(2)	1.394 (4)
P(1)–C(16)	1.760 (4)	C(1)–C(5)	1.388 (4)
P(1)–C(17)	1.771 (4)	C(2)–C(3)	1.404 (4)
F(61)–C(6)	1.334 (4)	C(2)–C(6)	1.479 (5)
F(62)–C(6)	1.325 (4)	C(3)–C(4)	1.400 (4)
F(63)–C(6)	1.322 (4)	C(3)–C(7)	1.475 (5)
F(71)–C(7)	1.343 (4)	C(4)–C(5)	1.410 (4)
F(72)–C(7)	1.345 (4)	C(4)–C(8)	1.480 (5)
F(73)–C(7)	1.334 (4)	C(5)–C(9)	1.475 (5)
F(81)–C(8)	1.343 (4)	C(10)–C(11)	1.385 (5)
F(82)–C(8)	1.345 (4)	C(10)–C(15)	1.390 (4)
F(83)–C(8)	1.328 (4)	C(11)–C(12)	1.389 (5)
F(91)–C(9)	1.344 (4)	C(12)–C(13)	1.377 (5)
F(92)–C(9)	1.341 (4)	C(13)–C(14)	1.360 (5)
F(93)–C(9)	1.340 (4)	C(14)–C(15)	1.385 (5)

Intramolecular Angles (deg)			
O(1)–P(1)–C(10)	107.8 (1)	C(2)–C(3)–C(4)	108.6 (3)
O(1)–P(1)–C(16)	110.9 (1)	C(2)–C(3)–C(7)	126.3 (3)
O(1)–P(1)–C(17)	106.7 (2)	C(4)–C(3)–C(7)	125.1 (3)
C(10)–P(1)–C(16)	112.1 (2)	C(3)–C(4)–C(5)	108.0 (3)
C(10)–P(1)–C(17)	109.3 (2)	C(3)–C(4)–C(8)	126.3 (3)
C(16)–P(1)–C(17)	109.9 (2)	C(5)–C(4)–C(8)	125.6 (3)
P(1)–O(1)–C(1)	124.1 (2)	C(1)–C(5)–C(4)	106.5 (3)
P(1)–C(10)–C(11)	118.6 (3)	C(1)–C(5)–C(9)	125.4 (3)
P(1)–C(10)–C(15)	121.0 (3)	C(4)–C(5)–C(9)	128.0 (3)
O(1)–C(1)–C(2)	124.1 (3)	C(11)–C(10)–C(15)	120.3 (3)
O(1)–C(1)–C(5)	125.4 (3)	C(10)–C(11)–C(12)	119.1 (3)
C(2)–C(1)–C(5)	110.4 (3)	C(11)–C(12)–C(13)	120.0 (4)
C(1)–C(2)–C(3)	106.3 (3)	C(12)–C(13)–C(14)	120.8 (3)
C(1)–C(2)–C(6)	125.9 (3)	C(13)–C(14)–C(15)	120.2 (3)
C(3)–C(2)–C(6)	127.8 (3)	C(10)–C(15)–C(14)	119.5 (3)

warming solutions of the kinetic adducts **3b–f** led to facile rearrangement to the analogous thermodynamic ylides **2b–f** (eq 3).



For instance, monitoring the rearrangement of **3b** to **2b** by ^{31}P NMR at 80 °C in toluene- d_6 showed a smooth conversion to the product in 10 h, as evidenced by the disappearance of the resonance at δ 27.6 for **3b** and appearance of a signal at δ 86.5 for **2b**. The ^{19}F NMR spectrum of **2b** shows two resonances of equal intensity at δ -49.8 and -51.0. The thermally induced rearrangements **3** \rightarrow **2** were found to be irreversible in the absence of light (vide infra).

The structure of the rearranged product **2b** was ascertained by X-ray diffraction analysis. Colorless rectangular blocks of this compound were obtained by slow evaporation of a CH_2Cl_2 solution at 25 °C. The ORTEP diagrams are shown in Figure 2A,B. Selected interatomic bond distances and angles for the extended conformational isomer (Figure 2A) are provided in Table II. The structure of the thermodynamic ylide **2b** is consistent with that proposed by Wilkinson and Roundhill⁶ for **2a**. A unique feature of the structure is the extremely long *c*-axis ($c = 56.862$ (4) Å) found for the unit cell (*Pbca* (no. 61)). The analysis showed that two different conformations of **2b** exist in the crystal, one with an extended arrangement (Figure 2A) and the other in a folded conformation with the phenyl group lying over the cyclopentadienyl (Cp) moiety (Figure 2B). These two conformations appear to arise from packing forces which allow the molecules to organize into separate sheets, each showing interactions between the phenyl groups and an adjacent Cp ring (see supplementary material). In general, the interatomic distances and angles are essentially the same for the two conformations. As expected, the cyclopentadienyl moiety of **2b** is planar, and the C–C distances within

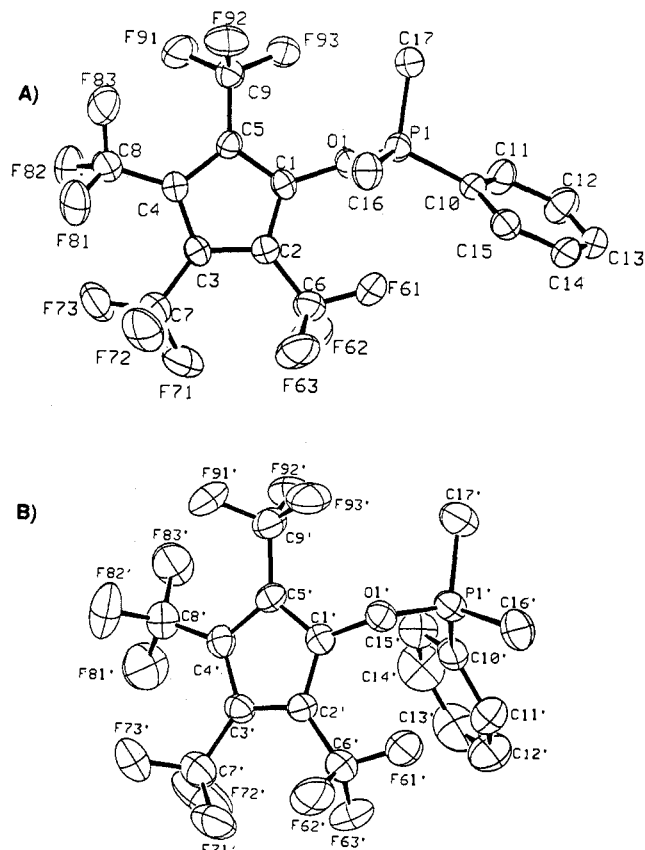


Figure 2. ORTEP plot of thermodynamic ylide **2b** with thermal ellipsoids drawn at the 50% probability level: (A) extended conformation and (B) folded conformation.

the five-membered ring are essentially equivalent (av C–C 1.40 Å). The C–O (1.409 Å) and P–O (1.584 Å) distance are normal for single bonds between these elements in this type of environment.⁹ In the folded conformation (Figure 2B), the phenyl group is slightly canted, and the closest intramolecular nonbonded C–C distance (3.140 Å) is between the ortho carbon C15' and C1' of the Cp ring.

The rearrangement **3** \rightarrow **2** also was found to be catalyzed by both Me_3SiCl and $n\text{-Bu}_4\text{NCl}$ at 25 °C. The addition of Me_3SiCl (1 equiv) to a CH_2Cl_2 solution of **3b** at 25 °C led to complete conversion to **2b** over 2 h; essentially no rearrangement to **2b** is observed under these conditions in the absence of Me_3SiCl over 24 h. A catalytic quantity (0.2 equiv) of Me_3SiCl also produces the ylide **2b** under these conditions, albeit at a slower rate (12 h). Similar results were obtained by using $n\text{-Bu}_4\text{NCl}$ as a catalyst, although the rates of product formation were slower than with Me_3SiCl . Synthetically, the use of Me_3SiCl as a catalyst for the rearrangement of **3** to **2** is the desired method for preparation of the ylides **2**; the mild reaction conditions lead to high product yield and purity.

The rate of the thermally induced rearrangement **3** \rightarrow **2** varied greatly with changes in the substituents on phosphorus (vide infra). Qualitatively, the kinetic adducts **3** containing small, electron-donating phosphines were found to be the most stable and resistant to rearrangement. In addition, heating toluene solutions of **3** in the presence of free phosphine resulted in greatly accelerated rates in the rearrangement to **2**. For example, treating a sample of **3b** in toluene with 1 equiv of PMe_2Ph at 80 °C led to complete conversion to **2b** in 30 min, indicating a 20-fold increase in the rate relative to no added phosphine. Prolonged heating of this solution showed the production of the known phosphorane Me_2PhPF_2 (^{31}P NMR δ -33, $J_{\text{PF}} = 592$ Hz) along with the disappearance of free PMe_2Ph and **2b**. In the absence of free

(9) Henrick, K.; Hudson, I. R.; Kow, A. *J. Chem. Soc., Chem. Commun.* 1980, 226.

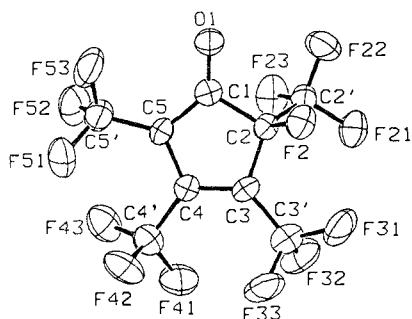
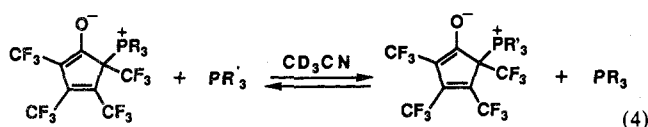


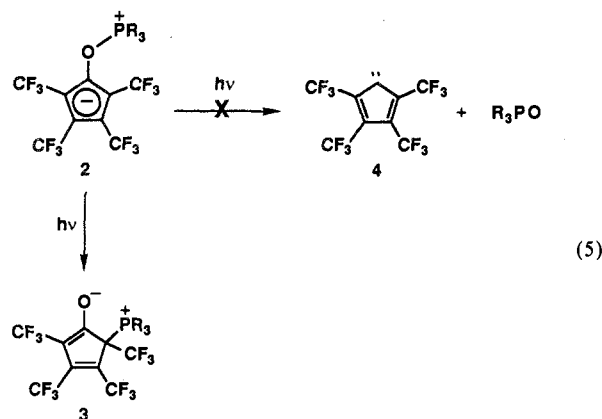
Figure 3. Molecular structure of fluoride adduct **5**. Thermal ellipsoids are drawn at the 50% probability level. TAS^+ counterion is omitted for clarity.

PMe_2Ph , no Me_2PhPF_2 was observed upon prolonged heating (80 °C, 24 h) of **2b**; higher temperatures ($T > 120$ °C) resulted in the decomposition of **2b** to uncharacterized products. Along similar lines, heating a C_6D_6 solution containing **3b** and 1 equiv of PET_3 at 80 °C for 30 min afforded a 1:1 mixture of **2b** and **2c**.

In the course of examining solvent effects, we have found that the thermal rearrangement $3 \rightarrow 2$ proceeds at a significantly slower rate in the polar solvent acetonitrile relative to the less polar aromatic hydrocarbon solvents. Surprisingly, the addition of free phosphine (PMe_3 , PET_3 , PMe_2Ph) to CH_3CN solutions of **3b-d** led not the expected accelerated rearrangement of **3** to **2** as seen above in toluene but to phosphine exchange over the temperature range 40–80 °C (eq 4). An equilibrium is approached from either direction relatively rapidly over the temperature range examined, and K_{eq} is approximately unity for the cases studied.



Photochemistry. Our interest in utilizing the ylides **2** as precursors to cyclopentadienide ligands led us to examine the photochemistry of these systems with the hope of photoextruding tertiary phosphine oxide and generating the known¹⁰ electrophilic carbene **4** (eq 5); Janulis and Arduengo¹⁰ have shown that **4** reacts with a variety of reagents to provide ylides and other cyclopentadiene derivatives.



Unexpectedly, subjecting a THF solution of the ylide **2b** ($\text{PR}_3 = \text{PMe}_2\text{Ph}$) in a quartz vessel to broad band irradiation (medium pressure Hg lamp) for 4 h at 25 °C resulted in complete conversion back to the kinetic adduct **3b**, which apparently (vide infra) is stable under these conditions (eq 5). Evidently an aromatic chromophore on phosphorus is not necessary for this transformation, as the PET_3 (**2c**) and PMe_3 (**2d**) ylides follow the same path upon irradiation. Prolonged irradiation (24 h) does not generate free phosphine oxide in these systems but instead leads

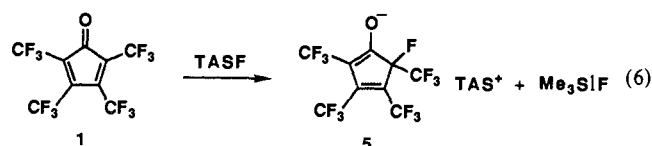
Table III. Selected Interatomic Distances (Å) and Intramolecular Angles (deg) for Fluoride Adduct **5**

Interatomic Distances (Å)			
F(2)–C(2)	1.388 (4)	F(53)–C(5')	1.319 (6)
F(21)–C(2')	1.335 (5)	O(1)–C(1)	1.225 (5)
F(22)–C(2')	1.317 (5)	C(1)–C(2)	1.562 (6)
F(23)–C(2')	1.335 (5)	C(1)–C(5)	1.404 (6)
F(31)–C(3')	1.322 (6)	C(2)–C(2')	1.518 (6)
F(32)–C(3')	1.352 (6)	C(2)–C(3)	1.500 (6)
F(33)–C(3')	1.349 (6)	C(3)–C(3')	1.475 (6)
F(41)–C(4')	1.329 (6)	C(3)–C(4)	1.346 (6)
F(42)–C(4')	1.318 (5)	C(4)–C(4')	1.514 (6)
F(43)–C(4')	1.335 (6)	C(4)–C(5)	1.428 (6)
F(51)–C(5')	1.362 (5)	C(5)–C(5')	1.465 (6)
F(52)–C(5')	1.347 (5)		

Intramolecular Angles (deg)			
F(2)–C(2)–C(1)	109.7 (3)	C(2)–C(3)–C(3')	122.6 (4)
F(2)–C(2)–C(2')	105.2 (4)	C(2)–C(3)–C(4)	106.9 (4)
F(2)–C(2)–C(3)	114.4 (3)	C(3')–C(3)–C(4)	130.5 (4)
O(1)–C(1)–C(2)	121.2 (4)	C(3)–C(4)–C(4')	124.3 (4)
O(1)–C(1)–C(5)	133.6 (4)	C(3)–C(4)–C(5)	113.4 (4)
C(2)–C(1)–C(5)	105.2 (4)	C(4')–C(4)–C(5)	122.3 (4)
C(1)–C(2)–C(2')	108.7 (3)	C(1)–C(5)–C(4)	109.1 (4)
C(1)–C(2)–C(3)	104.7 (4)	C(1)–C(5)–C(5')	122.8 (4)
C(2')–C(2)–C(3)	114.0 (4)	C(4)–C(5)–C(5')	128.0 (4)

to the phosphoranes F_2PR_3 , suggesting that free phosphine may be involved in these photochemical reactions. Irradiation of a THF solution containing **2b** and free PET_3 at 25 °C afforded a mixture of **3b** and **3c**. The incorporation of free PET_3 into **2b** to afford **2c** is not observed under these conditions, indicating that phosphine exchange in the starting material is not the source of **3c**. Phosphine exchange does occur, however, in the products **3** under the photochemical conditions. Irradiation of a THF solution containing **3b** and free PET_3 at 0 °C (no thermal phosphine exchange occurs at this temperature) yielded a mixture of **3b** and **3c** after 1 h.

(b) Fluoride. Treatment of TTFC (**1**) with the fluoride donor tris(dimethylamino)sulfonium trimethyldifluorosilicate (TASF)¹¹ cleanly afforded the crystalline fluoride adduct **5** as the TAS^+ salt (eq 6). Likewise, reaction between **1** and $n\text{-Bu}_4\text{NF}$



in THF leads to the analogous fluoride adduct as the tetrabutylammonium salt. Although spectroscopically similar, this compound proved difficult to purify, and further studies therefore were carried out on the TAS^+ salt **5**. The ^{19}F NMR spectrum of **5** indicated the presence of four inequivalent CF_3 groups and, by analogy with the phosphine adducts **3**, suggested the regiochemistry shown. The IR spectrum of **5** showed a $\text{C}=\text{O}$ stretch at 1660 cm^{-1} (^{13}C]-**5** showed the corresponding stretch at 1620 cm^{-1}), suggesting substantial double bond character in the carbonyl bond. Moreover, the ^{13}C NMR spectrum displayed a resonance at $\delta 181.0$ for the carbonyl group of **5**; this chemical shift is close to that for the carbonyl ^{13}C resonance of **1** ($\delta 183.0$).

The structure of the fluoride adduct **5** was elucidated by X-ray crystallography, and the ORTEP diagram is shown in Figure 3. The regiochemistry of fluoride addition to the α -carbon of **1** was confirmed. Selected interatomic distances and intramolecular angles are provided in Table III. Structural aspects of the TAS^+ cation are as expected based on previous studies¹² and will not be discussed. The ionic packing shows fairly well-separated ions, although the relatively short distance between C12 and F52 (3.14 Å) suggests the presence of a hydrogen-bonding interaction. The general structural features of **5** resemble those of the phosphine

(11) (a) Middleton, W. J. (to Du Pont) U.S. Patent 3,940,402, February, 1976. (b) Middleton, W. J. *Org. Synth.* **1985**, *64*, 221.

(12) Farnham, W. B.; Dixon, D. A.; Middleton, W. J.; Calabrese, J. C.; Harlow, R. L.; Whitney, J. F.; Jones, G. A.; Guggenberger, L. J. *J. Am. Chem. Soc.* **1987**, *109*, 476.

(10) Janulis, E. P., Jr.; Arduengo, A. J., III *J. Am. Chem. Soc.* **1983**, *105*, 3563.

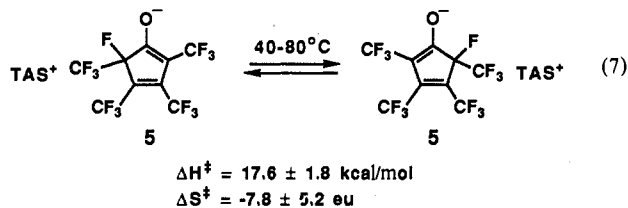
Table IV. Selected Interatomic Distances (Å) and Intramolecular Angles (deg) for Methanol Adducts *cis*-6a and *trans*-6a

Interatomic Distances (Å)			
O(1)–C(1)	1.197 (4)	C(4)–C(8)	1.527 (5)
O(2)–C(3)	1.376 (4)	C(5)–C(9)	1.497 (5)
O(2)–C(10)	1.421 (5)	C(11)–C(12)	1.510 (5)
O(11)–C(11)	1.196 (4)	C(11)–C(15)	1.489 (5)
O(12)–C(13)	1.394 (4)	C(12)–C(13)	1.552 (5)
O(12)–C(20)	1.440 (5)	C(12)–C(16)	1.508 (5)
C(1)–C(2)	1.517 (5)	C(13)–C(14)	1.545 (5)
C(1)–C(5)	1.500 (5)	C(13)–C(17)	1.536 (5)
C(2)–C(3)	1.556 (5)	C(14)–C(15)	1.318 (5)
C(2)–C(6)	1.507 (5)	C(14)–C(18)	1.502 (5)
C(3)–C(4)	1.535 (5)	C(15)–C(19)	1.512 (5)
C(3)–C(7)	1.543 (5)	C(2)–H(2)	0.940 (31)
C(4)–C(5)	1.329 (5)	C(12)–H(12)	0.876 (31)

Intramolecular Angles (deg)			
C(3)–O(2)–C(10)	116.2 (3)	C(3)–C(4)–C(5)	111.7 (3)
C(13)–O(12)–C(20)	118.3 (3)	C(3)–C(4)–C(8)	122.7 (3)
O(1)–C(1)–C(2)	128.0 (3)	C(5)–C(4)–C(8)	125.6 (4)
O(1)–C(1)–C(5)	126.9 (3)	C(1)–C(5)–C(4)	109.7 (3)
O(2)–C(3)–C(2)	115.7 (3)	C(1)–C(5)–C(9)	118.7 (3)
O(2)–C(3)–C(4)	117.9 (3)	C(4)–C(5)–C(9)	131.4 (4)
O(2)–C(3)–C(7)	102.8 (3)	C(12)–C(11)–C(15)	106.5 (3)
O(11)–C(11)–C(12)	127.8 (4)	C(11)–C(12)–C(13)	105.3 (3)
O(11)–C(11)–C(15)	125.7 (4)	C(11)–C(12)–C(16)	113.3 (4)
O(12)–C(13)–C(12)	115.1 (3)	C(13)–C(12)–C(16)	118.2 (4)
O(12)–C(13)–C(14)	114.0 (3)	C(12)–C(13)–C(14)	102.3 (3)
O(12)–C(13)–C(17)	104.3 (3)	C(12)–C(13)–C(17)	110.2 (3)
C(2)–C(1)–C(5)	105.0 (3)	C(14)–C(13)–C(17)	111.2 (3)
C(1)–C(2)–C(3)	103.0 (3)	C(1)–C(2)–C(6)	112.4 (3)
C(1)–C(2)–C(6)	115.8 (3)	C(13)–C(14)–C(18)	121.9 (3)
C(3)–C(2)–C(6)	122.4 (3)	C(15)–C(14)–C(18)	125.7 (3)
C(2)–C(3)–C(4)	101.0 (3)	C(11)–C(15)–C(14)	110.6 (3)
C(2)–C(3)–C(7)	112.3 (3)	C(11)–C(15)–C(19)	119.6 (4)
C(4)–C(3)–C(7)	107.2 (3)	C(14)–C(15)–C(19)	129.7 (4)

adducts **3**. The longer C–F bond distance associated with the fluorine attached to the ring (F(2)–C(2) = 1.388 Å) is probably a result of steric interactions with neighboring CF₃ groups. The C–O bond length of 1.22 Å is fairly normal for a carbonyl moiety of this sort⁸ and indicates that some negative charge may reside within the ring containing the CF₃ substituents. Also, as with the phosphine adducts **3**, the C–C bond distances around the five-membered ring suggest that a dienolate form similar to **3'** may best represent the electronic structure of **5**.

Fluorine Migration. We have discovered a rare example of what is formally a reversible 1,3-fluorine migration in the fluoride adduct **5** (eq 7). By using magnetization transfer techniques, we have



been able to monitor the migration of F between the two carbons adjacent to the carbonyl group of this compound. The rates for this process were measured over the temperature range of 40–80 °C, allowing a determination of the activation parameters: $\Delta H^\ddagger = 17.6 \pm 1.8 \text{ kcal/mol}$ and $\Delta S^\ddagger = -7.8 \pm 5.2 \text{ eu}$ with $\Delta G^\ddagger (60 \text{ }^\circ\text{C}) = 20.2 \pm 0.1 \text{ kcal/mol}$. Although sigmatropic fluorine migrations previously have been proposed,¹⁴ to our knowledge this

(13) Farnham, W. B.; Dixon, D. A.; Calabrese, J. C. *J. Am. Chem. Soc.* **1988**, *110*, 2607.

(14) (a) Kotaka, M.; Sato, S. *J. Fluorine Chem.* **1988**, *41*, 371 and references therein. (b) Bryce, M. R.; Chambers, R. D.; Taylor, G. *J. Chem. Soc., Chem. Commun.* **1983**, 1457. (c) Drayton, J. V.; Flowers, W. T.; Haszeldine, R. N.; Parry, T. A. *J. Chem. Soc., Chem. Commun.* **1976**, 490. (d) Bell, A. N.; Fields, R.; Haszeldine, R. N.; Kumadaki, I. *J. Chem. Soc., Chem. Commun.* **1975**, 866. (e) Feast, W. J.; Preston, W. E. *J. Chem. Soc., Chem. Commun.* **1974**, 985. (f) Camaggl, G.; Gozzo, F. *J. Chem. Soc. (C)* **1971**, 925.

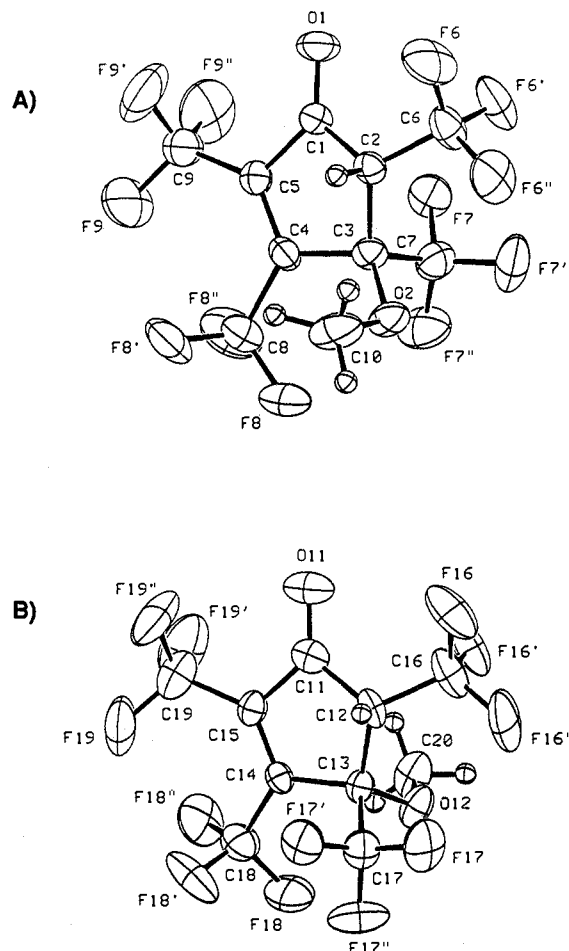
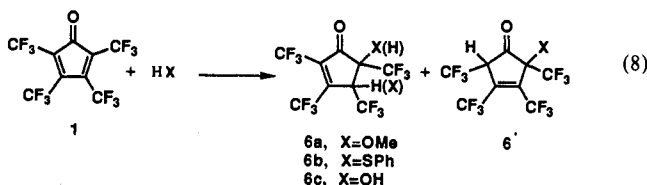


Figure 4. ORTEP drawings of methanol adducts **6a** with thermal ellipsoids drawn at the 50% probability level: (A) *cis* isomer (*cis*-6a) and (B) *trans* isomer (*trans*-6a).

is the first definitive example of a 1,3-fluorine shift in an anionic fluorocarbon; similar 1,2-fluorine migrations recently have been observed in related perfluorocarbanions.¹⁵ It is currently uncertain whether the mechanism of this process involves an intramolecular 1,3-fluorine shift, successive 1,2-fluorine migrations, or a dissociative pathway. No intermediate species were detected during our studies.

(c) **Protonic Nucleophiles.** It has been reported that the dienone **1** is unaffected by H₂O and MeOH.³ We, however, have found that treatment of **1** in Et₂O with a number of nucleophiles containing protons attached to the heteroatoms (HX) yielded products (**6**) derived from formal addition of HX across a double bond (eq 8). In the cases of methanol **6a** and thiophenol **6b**, the compounds



were isolated as colorless solids in good yield by solvent removal and sublimation (0.01 Torr, 40 °C) onto a –5 °C cold finger. Spectroscopic studies revealed the presence of an isomeric product mixture in both cases. While ¹⁹F NMR was most informative in determining the number of isomers present, it was often difficult to distinguish between the regioisomers **6** and **6'** and the corresponding stereoisomers. The protons attached to the rings of **6a–c** were shown to be rather acidic by the observation of rapid H/D

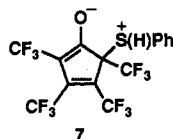
(15) Farnham, W. B., personal communication of unpublished results, 1989.

exchange with D₂O in solution.

The methanol adduct **6a** was isolated as a mixture of two isomers (~1:1), as determined by NMR spectroscopy. Slow crystallization of **6a** from a concentrated pentane solution at -20 °C afforded colorless which were suitable for X-ray analysis. The structure of **6a** was ascertained by crystallographic techniques, and the ORTEP drawings are provided in Figure 4. Interestingly, the crystal structure of **6a** consists of one *cis* isomer and one *trans* isomer per asymmetric unit. Selected interatomic bond distances and angles for both *cis*- and *trans*-**6a** are provided in Table IV. There are several notable structural features. In both isomers of **6a** the methoxy group is located on the β-carbon and the hydrogen is found (and refined) on the α-carbon of the cyclopentenone ring. The enone portion of the molecule is clearly marked by the observed short C=C (C4-C5 = 1.329 Å; C14-C15 = 1.318 Å) and C=O (C1-O1 = 1.197 Å; C11-O11 = 1.196 Å) bond distances. Both isomeric five-membered carbocycles have puckered (envelope) conformations with the α-carbons C2 and C12 deviating considerably from the planes of their respective rings. The isomers apparently prefer to pack together (1:1 occupancy) in the same crystal lattice rather than as isomerically pure individual crystals. Examination of the packing diagram (Figure 2S, supplementary material) shows the presence of a short intermolecular contact between the rather acidic *cis* H2 and a neighboring *trans* O11 (2.38 Å). A slightly weaker interaction is seen between *trans* H12 and a neighboring *cis* O1 (2.54 Å). It is possible that the formation of such hydrogen-bonding interactions is not as energetically favorable in the packing of isomerically pure molecules, thus explaining the preference for a mixed-isomer stacking motif.

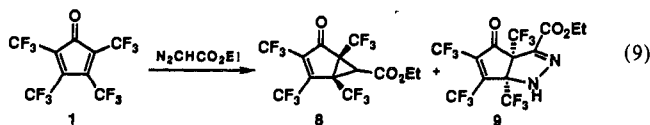
The reaction between **1** and methanol in CD₂Cl₂ does not take place to any great extent at low temperatures (*T* < 0 °C). Upon warming to 0 °C, a slow reaction takes place to afford a single isomeric product as determined by ¹H and ¹⁹F NMR measurements. Allowing the solution to stand at 25 °C for 24 h affords the ca. 1:1 mixture of isomers that are isolated upon sublimation and crystallization. The observation of facile isomerization in **6a** suggests that the observed regioisomer (OMe attached to the β-carbon of the ring) may have arisen from isomerization of an initial adduct formed by typical nucleophilic attack by the oxygen atom of MeOH at the α-carbon of **1**. Unfortunately, we obtained no evidence for the formation of a kinetic adduct in these systems.

By monitoring the reaction between **1** and thiophenol at -80 °C using ¹H and ¹⁹F NMR, we observed initial formation of a red adduct that displayed four ¹⁹F NMR resonances (δ -53.5, -57.5, -59.1, and -63.7) which, by analogy with the kinetic phosphine adducts **3**, we assign to **7**. This adduct was not one



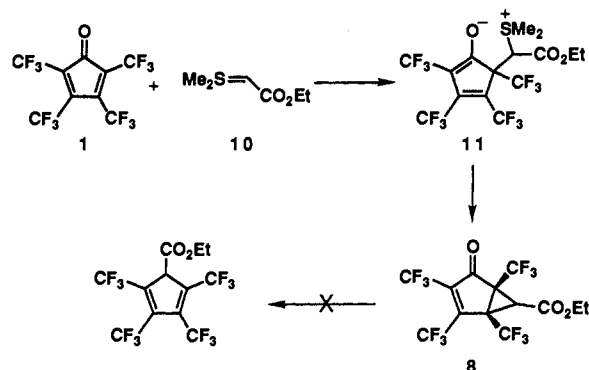
of the final products of the reaction. Upon warming to 25 °C, the solution became colorless, and the signals for **7** disappeared with concomitant growth of four new signals (see Experimental Section) associated with one of the isolated isomers of **6b**. Over 48 h in solution at 25 °C, further isomerization led to the same isomeric mixture that is isolated upon sublimation of **6b**.

(d) Ylide Addition. In line with our goal of utilizing **1** as a precursor to cyclopentadienyl compounds, we envisioned generating a cyclopropane derivative of TTFC which, under the proper conditions, could undergo vinylcyclopropane rearrangement and subsequent CO loss to afford the desired products. We, therefore, investigated the reaction between **1** and ethyldiazoacetate (Eq 9).



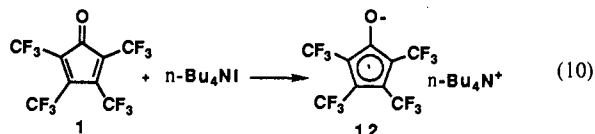
The reaction proceeded smoothly at 25 °C in the absence of a

Scheme I



catalyst to afford two products, **8** and **9**, which arise from cyclopropanation and 1,3-dipolar addition, respectively. The cyclopropane **8** was isolated as a colorless liquid in 20–30% yield; regardless of the conditions, the major product was **9** which was obtained as a colorless crystalline solid in 50–60% yield. Since, for our purposes, cyclopropane **8** was the desired product, an alternative route to this compound was sought. Treatment of TTFC (**1**) in hexane with the sulfur ylide **10**¹⁶ initially provided the product of nucleophilic addition (**11**) as a thermally sensitive colorless precipitate (8:1 mixture of diastereomers) (Scheme I). Allowing this sulfonium zwitterion (**11**) to stir in CH₂Cl₂ at 25 °C for 5 h resulted in Me₂S loss and production of the cyclopropane **8** in 70% isolated yield. For our purposes the synthesis of cyclopropane **8** apparently was for naught, however, since no conditions (pyrolytic or photochemical) could be found for the transformation of this compound into a cyclopentadiene derivative.

Radical Anion Salt. The success of fluoride addition to **1** to give the stable adduct **5** prompted us to examine the preparation of the chloride analogue by reaction with *n*-Bu₄NCl. Unexpectedly, the desired adduct could not be isolated. Instead, we obtained an orange solution containing a paramagnetic species which exhibited a 19-line EPR spectrum. The hyperfine coupling pattern suggested that the radical anion of **1** may have been generated, possibly through the oxidation of chloride ion. In order to further explore the production of a radical anion from **1**, we moved to the more reducing iodide. Reacting **1** with 1.5 equiv of *n*-Bu₄NI in CH₂Cl₂ afforded the stable, blue radical anion **12** as the tetrabutylammonium salt in 75% isolated yield (eq 10).



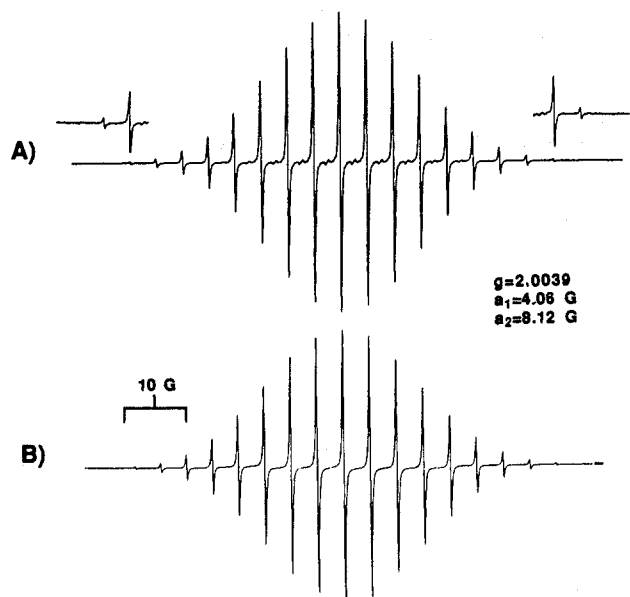
The EPR spectrum of **12** (Figure 5) in toluene or CH₂Cl₂ appears identical with that obtained upon reaction of **1** with chloride. The observed spectrum arises from hyperfine coupling between the unpaired spin and the fluorines of two inequivalent pairs of CF₃ groups. The *g* value (*g* = 2.0039) and magnitude of the hyperfine coupling constants (*a*₁ = 4.06 G, *a*₂ = 8.12 G) are most consistent¹⁷ with the unpaired electron being delocalized over the ring as shown for **12**, although the resonance structure with spin localization on oxygen and a stabilized aromatic anion cannot be ruled out completely. The expected septet of septets appears as a 19-line pattern as a result of one of the hyperfine coupling constants being exactly one-half the other. The calculated EPR spectrum of **12** (Figure 5B) was obtained from the experimental hyperfine coupling constants and is essentially identical with the observed spectrum. Magnetic susceptibility measurements on a crystalline sample of **12** using a Faraday balance showed the presence of a single unpaired spin (μ_{eff} = 1.65 μ_B). The IR spectrum of **12** in CH₂Cl₂ displayed three characteristic absorptions at 1580, 1534,

(16) Payne, G. B. *J. Org. Chem.* 1967, 32, 3351.

(17) Stock, L. M.; Wasielewski, M. R. In *Progress in Physical Organic Chemistry*; Taft, R. W., Ed.; John Wiley and Sons: New York, 1981; Vol. 13, pp 253–313.

Table V. Summary of X-ray Diffraction Data

	C ₁₇ H ₁₁ F ₁₂ OP (2b)	C ₁₅ H ₁₈ F ₁₃ N ₃ OS (5)	C ₁₂ H ₉ F ₁₂ OP (3d)	C ₁₀ H ₄ F ₁₂ O ₂ (6a)
formula	C ₁₇ H ₁₁ F ₁₂ OP (2b)	C ₁₅ H ₁₈ F ₁₃ N ₃ OS (5)	C ₁₂ H ₉ F ₁₂ OP (3d)	C ₁₀ H ₄ F ₁₂ O ₂ (6a)
symmetry	orthorhombic	monoclinic	monoclinic	triclinic
space group	<i>Pbca</i> (no. 61)	<i>P2₁/c</i> (no. 14)	<i>P2₁/n</i> (no. 14)	<i>P1</i> (no. 2)
<i>a</i> , Å	8.326 (1)	9.587 (6)	15.202 (2)	7.396 (1)
<i>b</i> , Å	15.941 (1)	11.864 (2)	11.579 (2)	11.174 (1)
<i>c</i> , Å	56.862 (4)	19.280 (20)	9.206 (4)	16.711 (2)
α , deg	90	90	90	71.67 (1)
β , deg	90	100.15 (3)	100.30 (2)	85.80 (1)
γ , deg	90	90	90	83.89 (1)
temp, °C	-70	-70	-100	-70
volume Å ³	7547.0	2158.6	1594.4	1302.4
<i>Z</i>	16	4	4	4
<i>F_w</i>	490.25	535.39	428.18	384.14
calcd density, g/cc	1.726	1.647	1.786	1.959
μ (Mo), cm ⁻¹	2.59	2.63	2.94	2.37
diffractometer	Enraf-Nonius CAD4	Enraf-Nonius CAD4	Syntex R3	Enraf-Nonius CAD4
radiation (graphite monochromator)	Mo K α	Mo K α	Mo K α	Mo K α
data collected	9646	4729	8050	6157
min. max 2 θ , deg	0.7, 55.0	2.1, 52.0	4.4, 55.0	2.6, 55.0
max <i>h, k, l</i>	10, 20, 73	11, 14, 23	19, 15, 11	9, 14, 21
data octants	+++	+++,-++	+++,-+-,-+-,-+-	+++,-+-,-+-,-+-
scan method	ω	ω	ω	ω
scan width, deg ω	0.9-1.20	1.20-1.90	1.00	1.20-1.80
scan speed, deg/min	1.30-5.00	1.70-5.00	3.90-19.50	1.70-5.00
typical half-height peak width, deg ω	0.20	0.14	0.33	0.22
check reflections	2, 54 times	2, 36 times	3, 44 times	2, 43 times
intensity variation	6.0% decrease	4% decrease	5.0% decrease	3% decrease
transmission factors			0.92-0.95	0.94-0.95
no. of unique data (<i>I</i> \geq 3.0 σ (<i>I</i>))	4268	2088	2445	2544
solution method	automated Patterson analysis	direct method (MULTAN)	direct methods (SHELXS)	direct methods (SHELXS)
anomalous terms	<i>P</i>	<i>S</i>	<i>P</i>	
weighting scheme	biweight $\propto [\sigma^2(I) + 0.0009I^2]^{-1/2}$	biweight $\propto [\sigma^2(I) + 0.0009I^2]^{-1/2}$	biweight $\propto [\sigma^2(I) + 0.0009I^2]^{-1/2}$	biweight $\propto [\sigma^2(I) + 0.0009I^2]^{-1/2}$
atoms refined	aniso: all non-hydrogen atoms fixed: H	aniso: all non-hydrogen atoms fixed: H	aniso: all non-hydrogen atoms iso: hydrogen atoms	aniso: all non-hydrogen atoms iso: hydrogen atoms
parameters varied	559	298	271	465
data/parameter ratio	7.62	6.98	9.00	5.47
<i>R</i> , <i>R_w</i>	0.048, 0.046	0.056, 0.051	0.036, 0.034	0.051, 0.038
error of fit	1.51	1.72	1.08	1.28
max shift Δ/σ	0.12	0.03	0.05	0.00
max residual density, e/Å ³	0.51	0.45	0.30	0.28

Figure 5. EPR spectra of radical anion salt **12** in toluene solution: (A) experimental spectrum and (B) calculated spectrum.

and 1515 cm⁻¹. The absorption band at 1515 cm⁻¹ may be assigned as a C-O stretch since ¹³C-labeled **12** (prepared by reducing [¹³C]-**1** with *n*-Bu₄NI) showed the expected isotopic red-shift for this absorption to 1499 cm⁻¹. The radical anion **12** was shown

to be relatively stable for short periods in air in the solid state and also was stable for more extended periods (48 h) in dry methylene chloride or toluene solution under N₂. Solutions of **12** do react rapidly with moisture and other electrophilic sources; details of this chemistry will be the subject of a future publication.¹⁸ The stability of the radical anion **12** led us to study the electrochemistry of **1**.

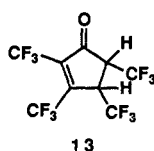
Electrochemistry of 1. Cyclic voltammetry experiments showed quasi-reversible redox behavior for **1** with a half-wave potential *E*_{1/2} = +0.37 V (vs SCE); coulometry indicated a one-electron reduction process. Bulk electrolysis at a standing potential of 0.0 V in CH₂Cl₂ generated a blue solution of the radical anion **12**. As expected, the EPR spectrum displayed by this solution was identical with that obtained for **12** synthesized by chemical means using iodide.

The large positive reduction potential for **1** suggested that, like the well-known organic oxidants 2,3-dichloro-5,6-dicyano-1,4-benzoquinone¹⁹ (*E*_{1/2} = 0.51 V vs SCE)²⁰ and tetracyanoethylene²¹ (*E*_{1/2} = 0.15 V vs SCE),²⁰ this compound may act as a good oxidizing reagent. Indeed, quantitative dehydrogenation of 1,4-cyclohexadiene to benzene and 9,10-dihydroanthracene to anthracene takes place upon reaction with **1**. The fluorine-containing product appears to arise from the addition of 1 mol-equiv of H₂ to **1** to give a single isomer (**13**) based on spectroscopic data; the

(18) Burk, M. J.; Krusic, P. J., manuscript in preparation.

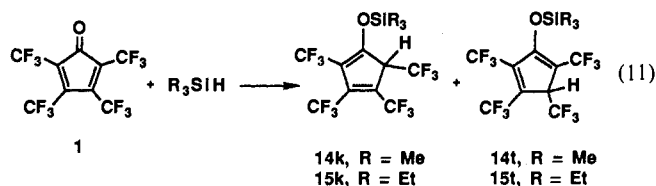
(19) Peover, M. J. *Chem. Soc. (London)* **1962**, 4540.(20) Ward, M. D. In *Electroanalytical Chemistry*; Bard, A. J., Ed.; Marcel Dekker, Inc.: New York, 1989; Vol. 16, p 181.(21) Garito, A. F.; Heeger, A. J. *Acc. Chem. Res.* **1974**, *7*, 232.

assignment of cis or trans stereochemistry is unclear. Reaction



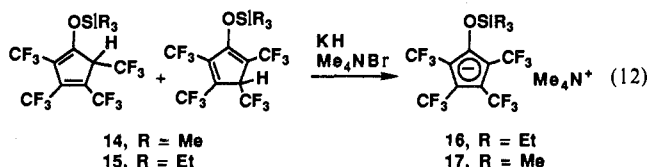
between **1** and 1,3-cyclohexadiene, on the other hand, affords no benzene but rather leads to the Diels–Alder adduct of **1**.⁴ Similarly, no dehydrogenation to benzene occurs, and instead a Diels–Alder adduct is observed, when 1,3-cyclohexadiene is treated with tetracyanoethylene.²² The demonstrated oxidizing power of **1** prompted us to investigate the interaction between **1** and potential transition-metal-based reductants.^{18,23,24}

Chemical Reduction. Siloxycyclopentadienides. An immediate reaction occurs upon treatment of TTFC (**1**) with trialkylsilanes in the absence of a catalyst (eq 11). The reduced products **14**



and **15** are obtained as a mixture of regioisomeric siloxydienes in 80–90% isolated yield. The ratio of isomers obtained varies with conditions such as temperature, reaction time, trace acid, etc. At low temperature ($\leq 0^\circ\text{C}$) the kinetic isomers **14k** and **15k** are obtained in >15:1 excess. Over 24 h in solution or over 15 min in the presence of trace acid, isomerization takes place to afford ~1:1 and 5:1 mixtures of **14t**:**14k** and **15t**:**15k**, respectively.

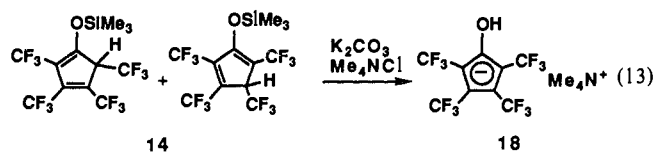
Treating a THF solution of the triethylsilane adducts **15** with KH in the presence of excess (5 equiv) Me_4NBr leads to deprotonation and generation of the new trifluoromethyl-substituted cyclopentadienyl derivative **16** as the tetramethylammonium salt in 75% yield (eq 12). The ^{19}F NMR spectrum of **16** shows a



single resonance for the CF_3 groups at $\delta -49.1$ ppm due to coincidental chemical shift overlap. The use of the cyclopentadienyl **16** as a ligand for transition metals has been communicated recently.⁵

Treatment of the (trimethylsilyloxy)dienes **14** with KH and Me_4NBr in THF affords predominantly the analogous (trimethylsilyloxy)cyclopentadienide **17** on the basis of NMR data. The trimethylsilyl groups in **14** and **17** are, however, extremely labile, thwarting attempts to cleanly separate the salt **17** from the obtained mixture. Due to the difficulties encountered in the purification of **17**, alternative routes to this compound with other counteranions were examined. We have found that treating the (trimethylsilyloxy)diene mixture **14** with $n\text{-Bu}_4\text{NBH}_4$ in CH_2Cl_2 led to deprotonation and afforded the cyclopentadienide **17b** as the tetrabutylammonium salt in good isolated yields.

Hydroxycyclopentadienide. Basic hydrolysis of the trimethylsilane adduct **14** with K_2CO_3 in wet THF containing excess (10 mol-equiv) Me_4NCl provides the novel hydroxycyclopentadienide salt $\text{Me}_4\text{N}^+[\text{C}_5(\text{CF}_3)_4(\text{OH})]^-$ (**18**) in 85% isolated yield (eq 13). The IR spectrum of **18** displays a broad O–H

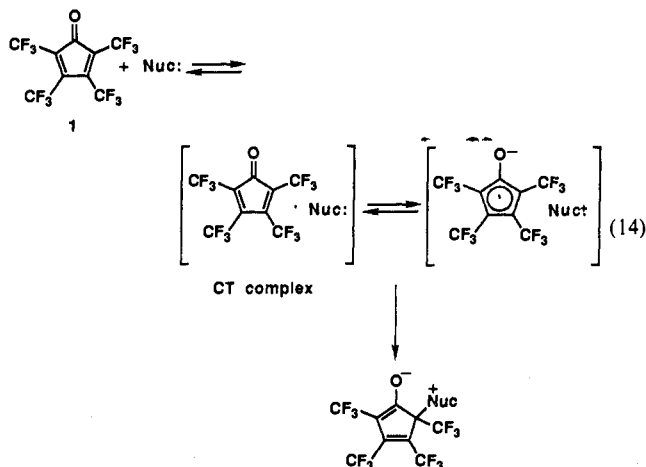


stretch at 3350 cm^{-1} . The ^1H NMR spectrum of **18** in $\text{THF-}d_6$ exhibits a broad resonance at $\delta 6.45$ ppm (1 H); rapid H/D exchange occurs with this proton upon the introduction of D_2O . The ^{19}F NMR spectrum shows two equal intensity signals at $\delta -49.3$ and -49.9 ppm for the two pairs of inequivalent CF_3 groups. Identical material was obtained under the same conditions from the (triethylsilyloxy)cyclopentadiene **15**. Likewise, reduction of **1** with 1 equiv of Me_4NBH_4 in THF also afforded the alcohol **18**, although in less pure form than described above by using **14**. Attempts to deprotonate the alcohol to generate the dianion led to decomposition, presumably through fluoride loss.

Discussion

Our original idea of utilizing tetrakis(trifluoromethyl)cyclopentadienone (**1**) as a direct precursor to a series of tetrakis(trifluoromethyl)cyclopentadienide derivatives via nucleophilic addition relied on the premise that the ylide **2a**⁶ was formed by kinetically controlled PPh_3 addition to the carbonyl oxygen of **1** (eq 1). Several experiments aimed at taking advantage of this mode of addition using other nucleophiles were not successful, which led us to reinvestigate the reactions between **1** and phosphines. Isolation of the kinetic phosphine adducts **3b–f** strongly suggested that the compound obtained by Wilkinson and Roundhill⁶ (**2a**) was not the kinetic product of PPh_3 addition but rather the thermodynamic product. Subsequent low-temperature NMR experiments confirmed the formation of betaine **3a** as the kinetic adduct resulting from Michael-type addition to **1**. These studies indicate that the electrophilic sites in **1** are at the carbon centers adjacent to the carbonyl group as expected for a dienone system and not at the oxygen atom, as was previously believed. Knowledge of this mode of reactivity associated with **1** subsequently led to the preparation of the desired cyclopentadienides by an alternative route involving reduction with trialkylsilanes.

Nucleophilic Addition. The addition of both soft (PR_3) and hard (F^-) nucleophiles to **1** generally was found to take place with regioselective kinetic attack at a carbon center adjacent to the carbonyl group. Although the regiochemistry observed in the isolated products suggests that a two-electron nucleophilic addition is the primary event, an initial one-electron process cannot be ignored. Given the demonstrated stability of the radical anion (**12**) derived from **1**, a plausible pathway for addition could proceed via initial one-electron oxidation of (or charge-transfer complex formation with) an incoming nucleophile to form the transient radical cation/radical anion (**12**) pair, followed by collapse to the products (eq 14). The formation of charge-transfer (CT) com-



plexes between **1** and various “nucleophilic” reagents such as olefins⁴ and arenes³ as well as amines³ previously has been noted

(22) Jacobson, B. M.; Soteropoulos, P.; Bahadori, S. *J. Org. Chem.* **1988**, *53*, 3247.

(23) Burk, M. J.; Tumas, W.; Ward, M. D.; Wheeler, D. M. *J. Am. Chem. Soc.* **1990**, *112*, 6133.

(24) Burk, M. J.; Staley, D. L.; Tumas, W. *J. Chem. Soc., Chem. Commun.* **1990**, 809.

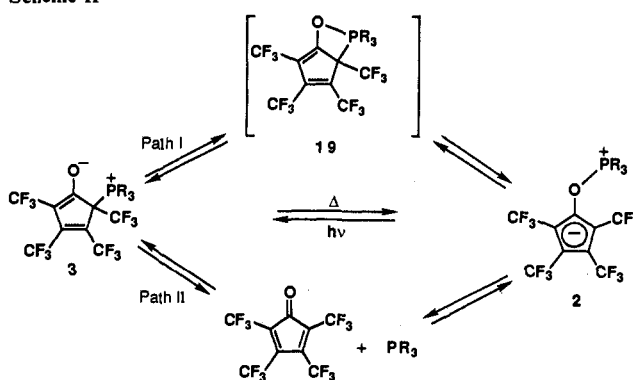
and is consistent with the possible intervention of a one-electron pathway in reactions involving **1**. The incorporation of a one-electron-transfer step into a "nucleophilic addition" mechanism involving **1** would indicate that the observed product regiochemistry is a result of selectivity in the radical ion combination step and not due to selective nucleophilic addition to the α -carbon of **1**. While the possibility of transient CT complex formation between **1** and phosphines appears real, the reaction between **1** and fluoride most likely involves a more conventional two-electron nucleophilic addition. The potential importance of radical-ion pathways in nucleophilic addition reactions has been a topic of great current interest.²⁵

Mechanism of the Rearrangement 3 \rightarrow 2. Rearrangement of the kinetic phosphine adducts **3** to the thermodynamic ylides **2** was shown to proceed readily under mild conditions. The relative rates of this rearrangement **3** \rightarrow **2** varied greatly with the substituents on phosphorus. For example, the PPh₃ adduct **3a** was observed by NMR to rearrange to **2a** at -50 °C, while the trimethylphosphine analogue **3d** was found to be relatively stable at 50 °C over several hours ($\sim 10\%$ conversion to **2d**). Both steric and electronic factors seem to be important in stabilizing the kinetic adducts **3**. Increasing the number of phenyl groups on phosphorus leads to a dramatic increase in the rate of rearrangement to **2**. While steric influences are probably partly responsible for the decreased stability of the PPh₃ ($\theta = 145^\circ$)²⁶ adduct **3a** relative to the PMe₂Ph ($\theta = 122^\circ$)²⁶ adduct **3b**, they are not the sole source of instability. This was clearly demonstrated by our ability to isolate the kinetic adduct **3f**, which contains the much more sterically demanding tricyclohexylphosphine (PCy₃, $\theta = 170^\circ$)²⁶; we were unable to isolate the analogous **3a** under any conditions. The electron-donating properties of the cyclohexyl groups on P appear to be great enough to overcome the unfavorable steric interactions in **3f**, thus allowing isolation of this compound. Increasing the number of alkyl groups on P apparently enhances its ability to stabilize the positive charge in the zwitterion **3**. The equal importance of steric interactions in determining the stability of the kinetic adducts **3**, however, was indicated by the mild conditions required for rapid rearrangement (10 min, 25 °C) of the kinetic adduct **3f** bearing the electron-donating yet sterically large tricyclohexylphosphine. In general, the kinetic adducts **3** were found to be most stable when electron-rich, sterically small phosphines were used.

Current mechanistic proposals concerning the Wittig reaction often invoke a stepwise process involving attack by a phosphorus ylide on a carbonyl compound to afford a betaine intermediate followed by rearrangement through a four-membered oxaphosphetane to provide as products the desired olefin and phosphine oxide.²⁷ Due to the betaine-like character of our kinetic phosphine adducts **3**, it was of interest to determine whether the rearrangement **3** \rightarrow **2** took place via an intramolecular mechanism (I) involving an oxaphosphetane intermediate (**19**) or through a dissociative intermolecular (II) pathway (Scheme II). A bimolecular pathway involving two molecules of **3** is also a mechanistic possibility for this rearrangement.

Several lines of evidence favor the dissociative mechanism (path II). First, heating a toluene solution of the kinetic PMe₂Ph adduct **3b** in the presence of free PET₃ (1 equiv) at 80 °C for 1 h led to a 1:1 mixture of the rearranged ylides **2b** and **2c**. While the exchange of PET₃ into starting **3b** to yield **3c** (and subsequently **2c**) was never observed under these conditions, such phosphine exchange in **3** was demonstrated to be a viable pathway in this reaction (vide infra). Therefore, a double-label crossover experiment was performed. Heating equimolar quantities of ¹³C-

Scheme II



labeled **3c** and unlabeled **3b** in toluene or THF at 80 °C resulted in complete scrambling of the ¹³C label into the products **2b** and **2c** as well as into the starting compound **3b**. No rearrangement or scrambling of the ¹³C label was observed when this experiment was performed at 25 °C. It is important to note at this time that all double-label crossover experiments were performed with materials that were recrystallized several times to insure the absence of adventitious free phosphine, which could catalyze phosphine exchange and produce the observed scrambling. The formation of the thermodynamic ylides **2** appears to be irreversible under thermal conditions; no scrambling of the ¹³C label was observed upon heating labeled ylide [¹³C]-**2b** and unlabeled **2c** in toluene at 80 °C for 12 h. Moreover, no triethylphosphine incorporation is observed upon heating (80 °C) the thermodynamic ylides **2a** or **2f** in the presence of free PET₃.

These experiments are suggestive but do not conclusively rule out a bimolecular pathway or a unimolecular mechanism involving an oxaphosphetane intermediate (path I) in the rearrangement. The possibility remains that rapid phosphine exchange occurs in **3** by an associative or dissociative pathway prior to unimolecular rearrangement to **2**. The addition of free phosphine (1 equiv) to warm (80 °C) toluene solutions containing the kinetic adduct **3b**, however, leads to ca. 20-fold increase in the rate of rearrangement to thermodynamic ylides **2**. This observed rate-accelerating effect of added phosphine in the rearrangement to **2** is inconsistent with a rate-limiting bimolecular (two molecules of **3**) or unimolecular (oxaphosphetane) process. Furthermore, the PCy₃ adduct **3f** was shown to rearrange to the thermodynamic ylide **2f** at 25 °C in THF. Performing this reaction in the presence free PET₃, however, yields exclusively the kinetic PET₃ adduct **3c** and no rearranged ylides. Subsequently heating this mixture to 70 °C affords a 1:1 mixture of the thermodynamic ylides **2c** and **2f**. Given the fact that **3c** is much more stable than **3f**, either a bimolecular reaction or unimolecular pathway proceeding through an oxaphosphetane intermediate (path I) would likely produce predominantly the PET₃ ylide **2c** with very little, if any, of the PCy₃ product **2f** being formed. This argument assumes that the hypothetical unimolecular rearrangements involving **3c** and **3f** would have comparable rates. In fact, given the similar electronic properties of PET₃ and PCy₃, the rate of formation of the postulated oxaphosphetane intermediates is likely to be much slower for **3f** due to the great steric demand of the PCy₃ moiety. Further studies showed that heating the PMe₂Ph kinetic adduct **3b** in the presence of free PCy₃ or PPh₃ (1 equiv) accelerates the rate of rearrangement and leads to 1:1 mixtures of the thermodynamic ylides **2b/2f** and **2b/2a**, respectively. Again, formation of the unstable PCy₃ and PPh₃ kinetic adducts would have to prevail in order for a bimolecular or unimolecular pathway to afford the obtained mixtures. The evidence presented above strongly suggests that the primary event in the thermal rearrangement **3** \rightarrow **2** involves initial, reversible P-C bond cleavage leading to **1** and free phosphine (dissociative path II), followed by irreversible nucleophilic attack at the oxygen atom of **1** to afford the thermodynamically stable ylides **2**.

In terms of the mechanism of the transformation **3** \rightarrow **2**, it was important to determine whether phosphine exchange in the kinetic adducts could be occurring in these reactions, and, if occurring,

(25) (a) Kochi, J. K. *Angew. Chem., Int. Ed. Engl.* **1988**, *27*, 1227. (b) Ashby, E. C. *Acc. Chem. Res.* **1988**, *21*, 414. (c) Chanon, M. *Acc. Chem. Res.* **1987**, *20*, 214. (d) Pross, A. *Acc. Chem. Res.* **1985**, *18*, 212. (e) Chanon, M.; Tobe, M. L. *Angew. Chem., Int. Ed. Engl.* **1982**, *21*, 1.

(26) (a) Tolman, C. A. *Chem. Rev.* **1977**, *77*, 313. (b) Rahman, Md. M.; Liu, H. Y.; Prock, A.; Geiring, W. P. *Organometallics* **1987**, *6*, 650.

(27) (a) March, J. *Advanced Organic Chemistry*, 3rd ed.; John Wiley and Sons, Inc.: New York, 1985; pp 845-854, and references therein. (b) Maryanoff, B. E.; Reitz, A. B. *Chem. Rev.* **1989**, *89*, 863.

whether it proceeds through a dissociative mechanism or via an S_N2' -type process where free PR_3 directly attacks the kinetic adducts **3**. As mentioned above, the thermal rearrangement $3 \rightarrow 2$ proceeded readily in toluene in the presence of added phosphine to give a 1:1 mixture of the ylides **2**. Warming solutions of **3b** and free triethylphosphine in the polar solvent acetonitrile, however, resulted in relatively little ($\sim 10\%$) rearrangement to the thermodynamic products **2**. Instead, phosphine exchange occurred under these conditions to give a mixture ($\sim 1:1$) of starting kinetic adducts **3b** and **3c**. As might be expected, heating a CH_3CN solution of **3b** and PPh_3 resulted in no apparent reaction, consistent with the relative instability of the kinetic PPh_3 adduct **3a**. A double-label crossover experiment was performed by heating ($80^\circ C$) an equimolar mixture of ^{13}C -labeled **3c** and unlabeled **3b** in CH_3CN . Scrambling of the ^{13}C label into **3b** was observed after 2 h, indicating that phosphine dissociation takes place readily under these conditions. On the basis of the experimental results above, it is apparent that phosphine exchange in acetonitrile most likely proceeds by a dissociative mechanism involving **1** and free phosphine. Invoking a dissociative mechanism for phosphine exchange is consistent with our previous findings which indicate that the same mechanism is operating in the thermal rearrangements $3 \rightarrow 2$. These results also suggest that the inhibitory effect of CH_3CN in the rearrangements $3 \rightarrow 2$ is likely due to greater dipole stabilization of the transition state leading to **3** relative to the transition state leading to **2** and not the result of stabilization of ground-state species **3**, since phosphine loss from **3** occurs readily in acetonitrile solution.

We have found that both Me_3SiCl and free chloride ($n-Bu_4NCl$) catalyze the rearrangement $3 \rightarrow 2$. Several experiments were performed in order to gain some information about the mechanism of this catalysis. Allowing an equimolar solution of the kinetic adduct **3b** and free PEt_3 to react with Me_3SiCl in CD_2Cl_2 at $25^\circ C$ (no phosphine exchange into the kinetic adducts **3** occurs at this temperature) results in a 1:1 mixture of the rearranged ylides **2b** and **2c**. Additionally, a double-label crossover experiment was performed and monitored by $^{13}C\{^{19}F\}$ NMR spectroscopy. Treating an equimolar mixture of ^{13}C -labeled **3b** and unlabeled **3c** in CD_2Cl_2 with Me_3SiCl or $n-Bu_4NCl$ at $25^\circ C$ resulted in a 1:1 mixture of ^{13}C -labeled ylides **2b** and **2c**. No incorporation of the ^{13}C label into **3c** was observed during these reactions, providing further evidence that no phosphine exchange occurs under these conditions. It is apparent that the catalysis is proceeding through a pathway involving initial cleavage of the P-C bond in **3** to afford some form of free PR_3 and **1**. Under the mild conditions of these experiments, reversion back to the kinetic adducts is expected. Apparently no back-reaction between this form of **1** and free PR_3 occurs, however, since no incorporation of free phosphine or scrambling of ^{13}C -label in **3** is observed. While the inducement of phosphine dissociation in the kinetic adducts **3** by Me_3SiCl and $n-Bu_4NCl$ appears certain, it is currently unclear what actual species are produced upon phosphine dissociation from **3** and why no back-reaction occurs under the mild conditions of these reactions. Furthermore, it is undetermined whether or not chloride ion is the catalyst operating in both systems, and additional mechanistic studies are required.

Photochemistry. Interestingly, irradiation of THF solutions containing the ylides **2** at $25^\circ C$ was shown to result in photo-reversion back to the kinetic adducts **3**. More detailed studies demonstrated the incorporation of added phosphine into the products; irradiation of the PMe_2Ph ylide **2b** and PEt_3 produced a mixture ($\sim 1:1$) of kinetic adducts **3b** and **3c**. In addition, complete scrambling of the ^{13}C -label in the products **3** was observed upon photolysis of an equimolar mixture of ^{13}C -labeled **2b** and unlabeled **2c**. These results suggest that P-O bond cleavage is the primary photochemical event in this system. Subsequent reaction between the photoproducts, free PR_3 and **1**, under the mild conditions of the photochemical experiment affords the kinetic phosphine adducts **3**. The kinetic adducts **3** also were found to be photochemically noninnocent. Irradiation of the kinetic zwitterions **3** in the presence of free phosphine PR_3 was found to result in phosphine exchange at $0^\circ C$, indicating that photo-

chemically induced P-C bond cleavage in **3** also readily occurs but in a reversible manner; no phosphine exchange occurs in the absence of light.

Summary. Our original goal of utilizing TTFC (**1**) for the preparation of trifluoromethyl-substituted cyclopentadienyl compounds required that we understand the reactivity of this molecule. The present studies have unveiled the multifaceted chemistry of **1** and eventually culminated in the preparation of several tetrakis(trifluoromethyl)cyclopentadienide salts (**16-18**). Reactions between TTFC and nucleophiles generally were shown to proceed in a Michael-type fashion with regioselective attack at an electrophilic carbon center adjacent to the carbonyl moiety of **1**. In the case of phosphines, the initially formed kinetic adducts (**3**) were shown to undergo facile thermally induced C to O rearrangement of PR_3 to yield the thermodynamic ylides (**2**). Irradiating the thermodynamic ylides (**2**) led to photoreversion back to the kinetic adducts (**3**). Mechanistic studies indicated that the rearrangements of **2** and **3** proceed through dissociative pathways involving P-O (photochemical) or P-C (thermal) bond cleavage, respectively. The analogous fluoride adduct **5** also was shown to be dynamic in solution, and magnetization transfer measurements allowed the rare observation of what is formally a reversible 1,3-fluorine migration.

In addition to two-electron reactions, TTFC also was shown to undergo transformations involving single-electron transfer. Electrochemical studies on **1** showed a reversible one-electron reduction wave at $E_{1/2} = 0.37 V$ (vs SCE), indicating that TTFC should prove to be a good, highly soluble one-electron chemical oxidizing agent.^{18,23,24} Consistent with this large positive reduction potential was our ability to isolate and characterize the stable radical anion salt **12** which was formed by reduction of **1** with iodide.

The results reported in this study help to clarify the relatively unexplored chemistry of the remarkable molecule tetrakis(trifluoromethyl)cyclopentadienone (**1**). As might be expected, the reactivity of this compound appears to be governed by the unique combination of great steric and electron-withdrawing properties associated with the four trifluoromethyl substituents of **1**. Our better understanding of the fascinating reactivity of TTFC and related derivatives has opened the door for future studies in this area.

Experimental Section

General Procedures. All manipulations were performed in a nitrogen-filled Vacuum Atmospheres Dri-Lab glovebox or by using standard Schlenk techniques. Benzene, toluene, diethyl ether (Et_2O), tetrahydrofuran (THF), glyme, hexane, and pentane were distilled from sodium-benzophenone ketyl under nitrogen. Acetonitrile (CH_3CN) and methylene chloride (CH_2Cl_2) were distilled from CaH_2 . Methanol was distilled from $Mg(OMe)_2$. Hexafluoro-2-butyne (Farchan), phosphines (Strem), and ^{13}CO (Isotec, Inc., Miamisburg, OH) were used as received.

Melting points were determined with a Mel-Temp apparatus in capillaries sealed under nitrogen and are uncorrected. Photochemical experiments were performed in quartz vessels at $25^\circ C$ or $0^\circ C$ with a broad band Hanovia 450 W (medium pressure) Hg lamp. NMR spectra were obtained on Nicolet NT-360 wide-bore (360 MHz 1H , 146 MHz ^{31}P , 339 MHz ^{19}F), Nicolet NT-300 wide-bore (300.75 MHz 1H , 121.74 MHz ^{31}P , 282.7 MHz ^{19}F , 75.63 MHz ^{13}C), and Nicolet QM-300 narrow-bore (300 MHz 1H) spectrometers. ^{13}C , ^{19}F , and ^{31}P NMR chemical shifts are positive downfield (and negative upfield) from external Me_4Si , $CFCl_3$, and 85% H_3PO_4 , respectively. IR spectra were recorded on a Nicolet 5DXB FT-IR spectrometer. EPR spectra were obtained on a Bruker ER-420 spectrometer. Magnetic susceptibility data were collected over the range 1.8-300 K with a Faraday balance. Elemental analyses were performed by Oneida Research Services, Inc., Whitesboro, NY, or Schwarzkopf Microanalytical Laboratory, Inc., Woodside, NY.

Tetrakis(trifluoromethyl)cyclopentadienone (1**).** Essentially following the published procedure³ with slight modifications, a 250-mL Hastelloy steel bomb was charged with $[Rh(CO)_2Cl]_2$ (8.0 g, 20.6 mmol) followed by hexafluoro-2-butyne (120 g, 0.714 mol). The vessel was then pressurized with 100 atm of CO and with continuous shaking was heated to $150^\circ C$ for 24 h. After cooling, the vessel was vented through a dry ice-cooled trap. The resulting brown residue was transferred from the bomb to a sublimation apparatus, and glass wool was placed on top to reduce splattering. Keeping the residue cold ($\sim 0^\circ C$), vacuum (0.1 Torr) was applied carefully. The sublimation was then conducted under

$J_{FF} = 6.5$ Hz, 3 F); ^{13}C NMR (CD_2Cl_2) δ 5.2 (CH_2), 6.3 (CH_3), 56.2 (CHCF_3), 120–125 (CF_3), 150–160 (CCF_3), 162.7 (COSiEt_3).

15t: ^1H NMR (CD_2Cl_2) δ 0.85 (q, $J_{\text{HH}} = 7.7$ Hz, 6 H), 1.01 (t, $J = 7.7$ Hz, 9 H), 4.48 (q, br, $J_{\text{HF}} = 6.6$ Hz, 1 H, rapid H/D exchange with D_2O); ^{19}F NMR (CD_2Cl_2) δ -55.63 (q, $J_{\text{FF}} = 6.1$ Hz, 3 F), -56.5 (sept, $J_{\text{FF}} = 9.1$ Hz, 3 F), -60.45 (q, $J = 10.4$ Hz, 3 F), -63.45 (dsept, $J_{\text{HF}} = 7.0$ Hz, $J_{\text{FF}} = 6.6$ Hz, 3 F).

(Triethylsiloxy)cyclopentadienide $\text{Me}_4\text{N}^+[\text{C}_5(\text{CF}_3)_4(\text{OSiEt}_3)]^-$ (**16**). The regioisomeric mixture **15k** and **15t** (1.6 g, 3.4 mmol) in THF (5 mL) was added dropwise to a mixture of KH (140 mg, 3.5 mmol) and Me_4NBr (2.63 g, 17.1 mmol) in THF (15 mL). Gas evolution (H_2) occurred throughout the addition, and the reaction was stirred for 40 min. The yellow mixture was then filtered through a Celite pad and concentrated to ~ 5 mL. Pentane (~ 40 mL) was added slowly to precipitate the product **16** as a fluffy white solid (1.35 g, 75%): ^1H NMR ($\text{THF}-d_6$) δ 0.70 (q, $J = 7.7$ Hz, 6 H), 0.92 (t, $J = 7.7$ Hz, 9 H), 3.0 (s, 12 H); ^{19}F NMR δ -49.1 (s, coincidental overlap of CF_3 groups); ^{13}C NMR δ 4.85 (CH_2), 6.0 (CH_3), 55.3 (CH_3N), 98.2 (CCF_3), 103.7 (CCF_3), 125.6 (CF_3), 126.1 (CF_3), 139.9 (COSiEt_3); assignments assisted by ^{19}F decoupling; ^{29}Si NMR ($\text{THF}-d_6$) δ +19.2. Anal. Calcd for $\text{C}_{19}\text{H}_{27}\text{F}_{12}\text{NOSi}$: C, 42.14; H, 5.02; N, 2.59. Found: C, 42.19; H, 4.94; N, 2.60.

(Trimethylsiloxy)cyclopentadienide $\text{Me}_4\text{N}^+[\text{C}_5(\text{CF}_3)_4(\text{OSiMe}_3)]^-$ (**17a**). The regioisomeric mixture of (trimethylsiloxy)dienes **14** (1.50 g, 3.5 mmol) in THF (5 mL) was added dropwise to a mixture of KH (0.141 g, 0.36 mmol) and Me_4NBr (2.70 g, 17.5 mmol) in THF (15 mL). Gas evolution immediately occurred, and, following the addition, the reaction was allowed to stir for 30 min. The yellow mixture was then filtered and concentrated to dryness. The residue was extracted with CH_2Cl_2 (25 mL) and filtered. The filtrate was concentrated to ~ 10 mL, and pentane was added to precipitate the product as a pale yellow solid (1.26 g, 72%): ^1H NMR ($\text{THF}-d_6$) δ 0.15 (s, 9 H, Me_3Si), 3.0 (s, 12 H, Me_4N); ^{19}F NMR ($\text{THF}-d_6$) δ -49.1 (s, CF_3 , coincidental overlap of signals). A suitable elemental analysis for **17** as the Me_4N^+ salt was not obtained.

(Trimethylsiloxy)cyclopentadienide $\text{Bu}_4\text{N}^+[\text{C}_5(\text{CF}_3)_4(\text{OSiMe}_3)]^-$ (**17b**). To the regioisomeric mixture of (trimethylsiloxy)dienes **14** (2.0 g, 4.7 mmol) in CH_2Cl_2 (5 mL) at -20 °C was added dropwise a solution of *n*- Bu_4NBH_4 . Gas evolution immediately occurred, and the solution remained pale yellow in color following the addition. The reaction was allowed to stir for 2 h at -20 °C and was then allowed to warm slightly over 5 min. To the yellow solution was added Et_2O (20 mL) and hexane (20 mL), and the cloudy mixture was cooled to -20 °C for 10 h. The resulting pale yellow precipitate was then filtered, washed with hexanes, and dried in vacuo. Recrystallization from CH_2Cl_2 /hexane afforded the product **17b** as a white crystalline solid (2.27 g, 73%): ^1H NMR ($\text{C}_2\text{D}_2\text{Cl}_2$) δ 0.15 (s, 9 H, Me_3Si), 1.0 (t, 12 H, CH_3), 1.4 (dq, 8 H, CH_2), 1.6 (dd, 8 H, CH_2), 3.0 (dd, 8 H, CH_2N); ^{19}F NMR (CD_2Cl_2) δ -49.1 (s, CF_3 , coincidental overlap of signals). Anal. Calcd for $\text{C}_{28}\text{H}_{45}\text{F}_{12}\text{N}_2\text{Si}$: C, 51.60; H, 6.96; F, 34.98; N, 2.15. Found: C, 51.66; H, 7.05; F, 34.89; N, 2.07.

Hydroxycyclopentadienide $\text{Me}_4\text{N}^+[\text{C}_5(\text{CF}_3)_4(\text{OH})]^-$ (**18**). A mixture of the (trimethylsiloxy)dienes **14** (3.0 g, 7.04 mmol) in THF (10 mL) was added dropwise to a vigorously stirred mixture of K_2CO_3 (1.95 g, 14.08 mmol) and Me_4NCl (7.70 g, 70.4 mmol) in wet THF (60 mL) at 0 °C. The pale yellow mixture was allowed to stir at 0 °C for 3 h. The insoluble salts were then filtered, and the filtrate was concentrated to ~ 10 mL. Hexane was added slowly with stirring to the filtrate, producing a colorless precipitate which was filtered, washed with pentane, and dried in vacuo. Recrystallization of this solid from CH_2Cl_2 /hexane afforded **18** as a colorless fluffy microcrystalline solid (2.41 g, 79%): mp (sealed capillary) 138–139 °C; ^1H NMR ($\text{THF}-d_6$) δ 2.97 (s, 12 H, CH_3), 6.45 (s (br), 1 H, OH, rapid H/D exchange with D_2O); ^{19}F NMR ($\text{THF}-d_6$) δ -49.3 (m, 6 F, CF_3), -49.85 (m, 6 F, CF_3). Anal. Calcd for $\text{C}_{13}\text{H}_{13}\text{F}_{12}\text{NO}$: C, 36.55; H, 3.07; F, 53.36; N, 3.28. Found: C, 36.82; H, 3.18; F, 53.21; N, 3.45.

Electrochemistry. Cyclic voltammetry experiments were performed in a standard H-cell with a glass-fritted separator with use of a Princeton Applied Research (PAR) potentiostat Model 173 with a PAR Universal Programmer Model 175 and a Hewlett Packard Model 7045 B X-Y recorder. Measurements were conducted on ca. 10^{-3} M substrate (**1**) in CH_2Cl_2 or CH_3CN at 25 °C in 0.1 M *n*- $\text{Bu}_4\text{N}^+\text{ClO}_4^-$ electrolyte by using Pt working and auxiliary electrodes. Bulk electrolyses were performed in CH_2Cl_2 at a fixed potential of 0.0 V vs Ag/AgCl. Oxidation potentials were determined vs a Bioanalytical Systems Ag/AgCl reference electrode and for comparison converted to SCF reference values. The reported potentials are referenced relative to the ferrocenium/ferrocene redox couple ($E^\circ = 0.41$ V vs SCE).

X-ray Crystallographic Analysis of 3d. Suitable crystals of the trimethylphosphine adduct **3d** were obtained by slow crystallization from a THF/ Et_2O solution at -40 °C. Crystal parameters and crystallo-

graphic data appear in Table V. A yellow rectangular plate of dimensions $0.39 \times 0.19 \times 0.41$ mm was mounted in a nitrogen-filled thin-walled glass capillary, and data were collected on a Syntex R3 diffractometer at -70 °C. The unit cell dimensions were determined by least-squares refinement of 48 reflections. Axial photographs about *a*, *b*, and *c* confirmed the lengths and symmetry of the axes. The crystal stability was monitored throughout the data collection by measuring the intensity of three standard reflections every 183 data points. The data were adjusted for a 5% decrease in intensity over the course of data acquisition. Lorentzian and polarization corrections as well as an empirical absorption correction based on ψ scan data were applied.

The structure was solved by using direct methods (SHELXS). Anisotropic refinement was carried out by full-matrix least squares on *F*. Neutral atom scattering factors were obtained from the *International Tables for X-ray Crystallography*, Vol. IV. Non-hydrogen atoms were refined anisotropically, and the hydrogens were refined isotropically for a total of 465 parameters. The refinement converged at $R = 0.036$, $R_w = 0.034$, and EOF = 1.08.

X-ray Crystallographic Analysis of 2b. Suitable crystals of the thermodynamic ylide **2b** were obtained by slow evaporation of a CH_2Cl_2 solution at 25 °C. Crystal parameters and crystallographic data appear in Table V. A colorless rectangular block of dimensions $0.45 \times 0.32 \times 0.45$ mm was mounted in a nitrogen-filled thin-walled glass capillary, and data were collected on an Enraf Nonius CAD 4 diffractometer at -70 °C. The unit cell parameters were determined by least-squares refinement of 25 reflections with 2θ between 16.8 and 33.2°. The *c*-axis was determined to be extremely long, $c = 56.862$ (4) Å. Remarkably the data appear unaffected by the long *c*-axis under the high-resolution conditions which were selected for this experiment. Axial photographs about *a*, *b*, and *c* confirmed the lengths and symmetry of the axes. The stability of the crystal was monitored throughout the data collection by measuring the intensity of two standard reflections every 179 data points. The data were adjusted for a 6% decrease in intensity over the course of data acquisition. Lorentzian and polarization corrections were applied, but no absorption correction was carried out due to the small absorption coefficient $\mu(\text{Mo}) = 2.59$ cm^{-1} .

The structure was solved with an automated Patterson analysis (PHASE). The asymmetric unit consists of two molecules in general positions. Hydrogen atoms were idealized with C–H = 0.95 Å. Anisotropic refinement was carried out by full-matrix least squares on *F*. Neutral atom scattering factors and anomalous scattering terms for *P* were obtained from the *International Tables for X-ray Crystallography*, Vol. IV. The refinement converged at $R = 0.048$, $R_w = 0.046$, and EOF = 1.51.

X-ray Crystallographic Analysis of 5. Suitable crystals of the fluoride adduct **5** were obtained by slow crystallization from a CH_2Cl_2 / Et_2O solution at -40 °C. Crystal parameters and crystallographic data appear in Table V. An irregular orange block of dimensions $0.47 \times 0.38 \times 0.52$ mm was mounted in a nitrogen-filled thin-walled glass capillary, and data were collected on an Enraf Nonius CAD 4 diffractometer at -70 °C. The unit cell dimensions were determined by least-squares refinement of 25 reflections with 2θ between 19.4 and 30.7°. Axial photographs about *a*, *b*, and *c* confirmed the lengths and symmetry of the axes. The crystal stability was monitored throughout the data collection by measuring the intensity of two standard reflections every 131 data points. The data were adjusted for a 4% decrease in intensity over the course of data acquisition. Lorentzian and polarization corrections were applied, but no absorption correction was carried out due to the small absorption coefficient $\mu(\text{Mo}) = 2.63$ cm^{-1} .

The structure was solved with direct methods (MULTAN). The asymmetric unit consists of one anion/cation pair in general positions. All hydrogen atoms on the methyl groups were determined from difference Fourier maps and idealized. Anisotropic refinement was carried out by full-matrix least squares on *F*. Neutral atom scattering factors and anomalous scattering terms for *S* were obtained from the *International Tables for X-ray Crystallography*, Vol. IV. Non-hydrogen atoms were refined anisotropically, and the hydrogens were refined isotropically for a total of 298 parameters. The refinement converged at $R = 0.048$, $R_w = 0.046$, and EOF = 1.51.

X-ray Crystallographic Analysis of 6a. Suitable crystals of the methanol adduct **6a** were obtained by slow crystallization from a concentrated pentane solution at -40 °C. Crystal parameters and crystallographic data appear in Table V. An irregular colorless block of dimensions $0.23 \times 0.24 \times 0.53$ mm was mounted in a nitrogen-filled thin-walled glass capillary, and data were collected on an Enraf Nonius CAD 4 diffractometer at -70 °C. The unit cell dimensions were determined by least-squares refinement of 25 reflections. Axial photographs about *a*, *b*, and *c* confirmed the lengths and symmetry of the axes. The crystal stability was monitored throughout the data collection by measuring the intensity of two standard reflections every 143 data points.

The data were adjusted for a 3% decrease in intensity over the course of data acquisition. Lorentzian and polarization corrections as well as an empirical absorption correction based on ψ scan data were applied.

The structure was solved with direct methods (SHELXS). The asymmetric unit consists of one cis isomer and one trans isomer of **6a** in general positions. Anisotropic refinement was carried out by full-matrix least squares on F . Neutral atom scattering factors were obtained from the *International Tables for X-ray Crystallography*, Vol. IV. Non-hydrogen atoms were refined anisotropically, and the hydrogens were refined isotropically for a total of 465 parameters. The refinement converged at $R = 0.051$, $R_w = 0.038$, and EOF = 1.28.

Acknowledgment. We thank J. E. Feaster, L. Lardear, and W. Marshall for expert technical assistance. We also thank J. Lazar for obtaining HRMS spectra, R. S. McLean for magnetic sus-

ceptibility data, E. Conaway for ^{31}P and ^{19}F NMR data, and W. Barney for EPR spectra. We are grateful to Dr. M. D. Ward for performing electrochemical experiments, Dr. P. J. Krusic for simulating the EPR spectrum of **12**, and Drs. A. J. Arduengo, III, and B. E. Smart for helpful discussions.

Supplementary Material Available: Tables of final positional and isotropic thermal parameters, anisotropic thermal parameters, complete interatomic bond distances, and complete intramolecular bond angles for **2b**, **3d**, **5**, and **6a**, additional ORTEP plots for **2b**, **3b**, and **5**, and packing diagrams for **2b**, **5**, and **6a** (23 pages); tables of observed and calculated structure factors for **2b**, **3d**, **5**, and **6a** (31 pages). Ordering information is given on any current masthead page.

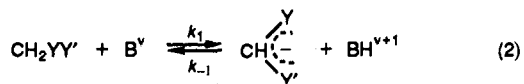
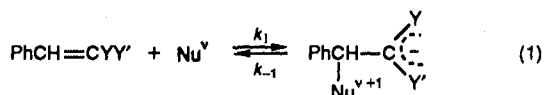
Kinetics of Amine Addition to Benzylidene-1,3-indandione and Other Vinylic β -Diketones. Effect of Cyclic Structure and Steric Strain on Intrinsic Rate Constants

Claude F. Bernasconi* and Michael W. Stronach

Contribution from the Department of Chemistry and Biochemistry, University of California, Santa Cruz, California 95064. Received October 9, 1990

Abstract: The kinetics of the reactions of benzylidene-1,3-indandione (**4**) with piperidine, morpholine, *n*-butylamine, 2-methoxyethylamine, glycineamide, and cyanomethylamine and the reactions of benzylidene-3,5-heptanedione (**5**), benzylidene-2,6-dimethyl-3,5-heptanedione (**6**), and benzylidenedibenzoylmethane (**7**) with piperidine and morpholine have been measured in 50% Me_2SO -50% water (v/v) at 20 °C and 0.5 M ionic strength. The reactions lead, in all cases, to the reversible formation of the zwitterionic adduct $\text{PhCH}(\text{RR}'\text{NH}^+)\text{C}(\text{COX})_2^-$ (T_A^\ddagger) that is in fast equilibrium with its anion $\text{PhCH}(\text{RR}'\text{N})\text{C}(\text{COX})_2^-$ (T_A^-). Rate constants for nucleophilic addition (k_1) and its reverse (k_{-1}) as well as the pK_a of T_A^\ddagger were determined for all reactions. The intrinsic rate constant ($k_0 = k_1 = k_{-1}$ when $K_1 = 1$) for amine addition to **4** is abnormally high, whereas k_0 for the reactions of **5-7** are abnormally low and similar to k_0 in magnitude for amine addition to benzylideneacetylacetone reported previously. The terms "abnormally high" and "abnormally low" refer to positive and negative deviations, respectively, from a plot of $\log k_0$ for amine addition to a series of electrophilic olefins of the type $\text{PhCH}=\text{CYY}'$ vs $\log k_0$ for deprotonation of carbon acids of the type $\text{CH}_2\text{YY}'$. The high k_0 for the reaction of **4** is attributed to its cyclic structure, which assures that the π -overlap required for the stabilization of the adduct is strongly developed in the transition state. The low k_0 values for the reactions of **5-7** arise from intramolecular hydrogen bonding, which is strong in T_A^\ddagger but poorly developed in the transition state, and from steric strain in the adduct, which is strongly developed in the transition state. All these effects can be viewed as manifestations of the principle of nonperfect synchronization (PNS).

Previous work has shown that the rates of reversible nucleophilic addition to electrophilic olefins (eq 1) are governed by factors similar to those that govern the rates of deprotonation of carbon acids (eq 2).¹ This becomes especially apparent when, for a given YY' , the *intrinsic* rate constants (k_0) for reactions 1 and 2 (k_0



$= k_1 = k_{-1}$ when $K_1 = 1$)^{2,3} are compared to one another. For both types of reactions, k_0 decreases with increasing resonance

stabilization of the carbanionic product, i.e., in the order $\text{CN}, \text{CN} \gg (\text{COO})_2\text{C}(\text{CH}_3)_2^{\text{3a}} \gg \text{CN}, \text{C}_6\text{H}_4\text{-4-NO}_2 \sim \text{C}_4\text{Cl}_4^{\text{5b}} > \text{CN}, \text{C}_6\text{H}_3\text{-2,4-(NO}_2)_2 > \text{H}, \text{NO}_2 > \text{C}_6\text{H}_5, \text{NO}_2$.

In fact, a plot of $\log k_0$ for piperidine and morpholine addition to $\text{PhCH}=\text{CYY}'$ ($\log k_{0\text{N}}$) in 50% Me_2SO -50% water vs $\log k_0$ for deprotonation of $\text{CH}_2\text{YY}'$ by piperidine and morpholine ($\log k_{0\text{P}}$) in the same solvent is well-approximated by a straight line of slope 0.46 ± 0.07 (Figure 1). The decrease in $(k_0)_\text{P}$ and $(k_0)_\text{N}$ with increasing resonance in the carbanion has been interpreted as being primarily a manifestation of the principle of nonperfect synchronization (PNS)^{1,6} and linked to imbalanced transition states in which the development of resonance lags behind charge transfer or bond formation. According to the PNS, a product stabilizing factor (in this case, resonance) that develops late along the reaction coordinate always lowers k_0 .⁷

Figure 1 shows one strongly deviant point: $(k_0)_\text{N}$ for benzylideneacetylacetone (**1**)⁸ is about 2.5 log units smaller than ex-

(1) (a) Bernasconi, C. F. *Acc. Chem. Res.* **1987**, *20*, 301. (b) Bernasconi, C. F. *Tetrahedron* **1989**, *45*, 4017.

(2) For proton transfers, statistical factors are usually included and $\log(k_0)_\text{P}$ is defined as $\log(k_1/q)$ when $\log K_1 + \log(p/q) = 0$, where p is the number of protons on $\text{BH}^{\nu+1}$ and q is the number of equivalent basic sites on B^ν .

(3) Regarding potential problems with the definition of k_0 for an addition reaction due to different units for k_1 and k_{-1} , see ref 4.

(4) Bernasconi, C. F. *Adv. Phys. Org. Chem.* **1991**, *27*, in press.

(5) (a) $\text{CH}_2(\text{COO})_2\text{C}(\text{CH}_3)_2$ is Meldrum's acid. (b) $\text{CH}_2\text{C}_4\text{Cl}_4$ is 1,2,3,4-tetrachloro-1,3-cyclopentadiene.

(6) Bernasconi, C. F. *Tetrahedron* **1985**, *41*, 3219.

(7) A corollary to the original formulation of the PNS is that a product-stabilizing factor that develops early increases k_0 . Alternatively, a product-destabilizing factor that develops early decreases k_0 ; one that develops late increases k_0 .